10/7-18-90 OSD

SANDIA REPORT

SAND86—0558
Unlimited Release
Printed May 1990

Yucca Mountain Project

Preliminary Laboratory Testing of Selected Cementitious Material for the Yucca Mountain Project Repository Sealing Program

P. H. Licastro, J. A. Fernandez, D. M. Roy

DO NOT MICROFILM COVER

Prepared by
Sandia National Laboratories
Albuquerque, New Mexico 87185 and Livermore, California 94550
for the United States Department of Energy
under Contract DE-AC04-76DP00789

DISTRIBUTION OF THIS DOCUMENT IS UNLIMITED

DISCLAIMER

This report was prepared as an account of work sponsored by an agency of the United States Government. Neither the United States Government nor any agency thereof, nor any of their employees, makes any warranty, express or implied, or assumes any legal liability or responsibility for the accuracy, completeness, or usefulness of any information, apparatus, product, or process disclosed, or represents that its use would not infringe privately owned rights. Reference herein to any specific commercial product, process, or service by trade name, trademark, manufacturer, or otherwise does not necessarily constitute or imply its endorsement, recommendation, or favoring by the United States Government or any agency thereof. The views and opinions of authors expressed herein do not necessarily state or reflect those of the United States Government or any agency thereof.

DISCLAIMER

Portions of this document may be illegible in electronic image products. Images are produced from the best available original document.

"Prepared by Yucca Mountain Project (YMP) participants as part of the Civilian Radioactive Waste Management Program (CRWM). The YMP is managed by the Yucca Mountain Project Office of the U.S. Department of Energy, Nevada Operations Office (DOE/NV). YMP work is sponsored by the Office of Geologic Repositories (OGR) of the DOE Office of Civilian Radioactive Waste Management (OCRWM)."

Issued by Sandia National Laboratories, operated for the United States Department of Energy by Sandia Corporation.

NOTICE: This report was prepared as an account of work sponsored by an agency of the United States Government. Neither the United States Government nor any agency thereof, nor any of their employees, nor any of their contractors, subcontractors, or their employees, makes any warranty, express or implied, or assumes any legal liability or responsibility for the accuracy, completeness, or usefulness of any information, apparatus, product, or process disclosed, or represents that its use would not infringe privately owned rights. Reference herein to any specific commercial product, process, or service by trade name, trademark, manufacturer, or otherwise, does not necessarily constitute or imply its endorsement, recommendation, or favoring by the United States Government, any agency thereof or any of their contractors or subcontractors. The views and opinions expressed herein do not necessarily state or reflect those of the United States Government, any agency thereof or any of their contractors.

Printed in the United States of America. This report has been reproduced directly from the best available copy.

Available to DOE and DOE contractors from
Office of Scientific and Technical Information
PO Box 62
Oak Ridge, TN 37831

Prices available from (615) 576-8401, FTS 626-8401

Available to the public from
National Technical Information Service
US Department of Commerce
5285 Port Royal Rd
Springfield, VA 22161

NTIS price codes
Printed copy: A05
Microfiche copy: A01

SAND86-0558
Unlimited Release
Printed May 1990

SAND--86-0558

DE90 013554

PRELIMINARY LABORATORY TESTING OF SELECTED CEMENTITIOUS MATERIAL FOR THE YUCCA MOUNTAIN PROJECT REPOSITORY SEALING PROGRAM

P. H. Licastro*
J. A. Fernandez+**
D. M. Roy*

*Materials Research Laboratory
The Pennsylvania State University
University Park, PA

+Geoscience Assessment and
Validation Division
Sandia National Laboratories
Albuquerque, NM

ABSTRACT

This report presents the results from laboratory tests on cementitious materials in support of the Yucca Mountain Project repository sealing program. The first part of this study included the short-term determination of physical and mechanical properties of eight mixtures. From this study, two expansive mixes--one grout and one mortar--were selected for more extensive study, which included mechanical properties over an extended period of time (2 yr) as well as interface permeability and bond strength measurements. As a further extension of this study, an additional mix was formulated to reduce the sulfate content with the objective of lessening the potential of sulfate reacting as a complexing agent. Short-term mechanical properties of this mix were also determined. Data reflecting the physical and mechanical properties of the above cementitious mixtures indicate that potentially suitable cementitious sealing materials can be developed for use in a repository located in an unsaturated tuff environment. However, additional laboratory testing will be required to more completely understand the basic properties of potentially suitable cementitious mixtures in an unsaturated tuff environment. Also, the suitability of each lab test should be evaluated to determine if reliable material property values can be obtained from the test.

MASTER

DISTRIBUTION OF THIS DOCUMENT IS UNLIMITED

QA Level of Work

Because this work was performed before the existence of an approved Yucca Mountain Project QA plan, no quality level is designated to this work. Therefore, the data presented in this report will not be used directly to support the License Application Design. The purpose of conducting this work was three-fold: (1) to provide a better understanding of difficulties encountered in laboratory testing; (2) to support the preparation of the study plan for sealing defined in the Site Characterization Plan (DOE, 1988); and (3) to gain a basic understanding of the representative material properties for grouts and mortars. Because of the intended use of this report, the results given here are considered to be scoping only and to be used for planning the sealing program. As such this report is not intended to answer all of the technical questions that arose during the performance of this work. Future testing will be performed as part of the Yucca Mountain Project repository sealing program to support the License Application Design.

The results presented in this report were obtained through three separate contracts and organizations. The short-term characterization of grouts and mortars (Phase I) was controlled by the Battelle Project Management Division, Office of Nuclear Waste Isolation. The long-term characterization of the two materials evaluated in Phase II was controlled by Sandia National Laboratories. All geochemistry aspects of Phase II work were controlled by Los Alamos National Laboratory (LANL). LANL was also responsible for the extended testing conducted as part of Phase II work.

CONTENTS

CONTENTS
(Concluded)

FIGURES

TABLES

TABLES
(Concluded)

1.0 INTRODUCTION

The Yucca Mountain Project, managed by the Nevada Operations Office of the U.S. Department of Energy, is composed of a variety of activities including waste package design; geologic, geochemical, and hydrologic studies; repository design; and repository sealing. These studies are focusing on the tuffs of the Yucca Mountain area. The Topopah Spring Member of the Paintbrush Tuff has been identified by Johnstone et al. (1984) as the most suitable geologic unit of the area in which to locate a repository for disposal of radioactive wastes, which would potentially include commercial and defense high-level wastes and spent fuel. The prospective repository is located in the unsaturated zone and in welded tuff.

The work presented here is part of the materials evaluation portion of the Yucca Mountain Project repository sealing program (Fernandez, 1985). Sandia National Laboratories is responsible for integrating the materials evaluation efforts with the seal performance/requirements, field testing, and seal design portions of the sealing program. Pennsylvania State University (PSU) and Los Alamos National Laboratory were given the task of performing scoping laboratory analyses to determine material properties of selected mortars and grouts. These properties included physical, mechanical, and geochemical properties of potential sealing materials.

The strategy adopted in the Yucca Mountain Project repository sealing program is to evaluate the properties of the potential seal materials concurrently with the development of sealing concepts and sealing requirements. Consistent with this strategy, a materials evaluation effort was initiated to identify sealing materials that could be suitable in an unsaturated tuff environment. Because no specific design requirements for a repository in the unsaturated tuff environment were available when testing began, it was decided to obtain an initial data base of properties of sealing materials that could be used to support the sealing design effort and future laboratory testing effort. The focus was on cementitious materials because they are versatile construction materials and have well-established characteristics.

This report describes the mechanical and physical properties of potential grout and mortar formulations. A companion report (Scheetz and Roy, 1989) describes the chemical characteristics of selected material formulations. A broad range of mechanical and physical properties were measured to provide a broad data base for the materials studied. The properties that were measured include

- interface permeability, i.e., the permeability between the host rock and the seal material;
- compressive strengths;

- permeability of the seal material;
- bond strength between the seal material and the host rock;
- expansivity of the seal material;
- volume stability; and
- thermal conductivity.

This report presents the logic used in formulating the seal materials and the results from the laboratory testing of the grouts and mortars. The work was carried out in two phases: a preliminary screening phase (Phase I), generic in nature, was followed by a site-specific, more extensive evaluation (Phase II) of the physical and mechanical properties (over an extended period of time) for two of the more promising preliminary candidate formulations that achieve some qualitative criteria. These criteria were moderate strength, low matrix permeability, low interface permeability, and adequate workability. As an extension of Phase II, an additional mix was formulated and tested. This mix was designed to reduce the sulfate content of the seal material, thereby reducing the potential for transport of radionuclides. Short-term mechanical properties of these mixes were also determined. Because of the preliminary nature of this work, more evaluations of the properties of sealing material will be performed before seal design.

2.0 APPROACH

The preliminary screening phase (Phase I) consisted of the formulation and testing of mixes representing mortars and grouts, both expansive and nonexpansive, with bulk compositions approaching those of tuff. Short-term evaluation of these mixes included the determination of physical/mechanical properties as a function of time (up to 28 days) and curing temperature (38 and 60°C). Ancillary data included characterization of starting materials, phase identification, and limited interface experimentation, i.e., bond strength and permeability, using a nonwelded tuff, which was available when testing was initiated. Unless otherwise noted, samples used to measure unconfined compressive strengths, bulk density, porosity, thermal conductivity, permeability of the seal material, and interface permeability were stored by immersion in water following an initial curing time in a high-humidity room (>95% relative humidity). Samples for bond strengths were stored in a >95% relative humidity room. Viscosity and dimensional stability measurements were done on samples in a plastic state.

The eight mixes designated for Phase I testing were formulated considering the bulk chemical composition of tuff. These mixes were modified by the type and proportion of starting materials to provide grouts and mortars with minimal shrinkage characteristics. Details of the starting materials used for these formulations are presented in Table 1. The bulk chemistry of the formulations is shown in Figure 1, a ternary diagram showing the bulk chemistry of the studied materials and mixtures normalized with respect to CaO, Al_2O_3, and SiO_2, the major constituents of cement. The chemical compositions of two categories of tuff are also displayed in Figure 1. Both categories of tuff are used in the studies presented in this report. Welded tuff samples were obtained from the Topopah Spring Member (Busted Butte outcrop) and nonwelded tuff samples were obtained from the Grouse Canyon Member in G-Tunnel. The locations of Busted Butte, G-Tunnel, and Yucca Mountain are shown in Figure 2. Although the crystalline, welded tuffs (from the Busted Butte outcrop) and the nonwelded zeolitized tuffs (from G-Tunnel*) may differ in mineralogy and petrology, their weight percentage of CaO, SiO_2, and Al_2O_3 are similar. Therefore, development of cementitious material similar to the bulk chemistry for a welded or nonwelded tuff would be the same.

Class H cement was the primary cementitious constituent in six of the preliminary mixtures. The coarse grind of this cement provides lower rates of reaction and heat generation and permits the use of low water-to-cement

---

*Nonwelded, zeolitized tuffs were selected from G-Tunnel to support the interface permeability and bond strength measurements for Phase I testing discussed in this report. Tuff from G-Tunnel was selected because it was readily available, and at the time this work was initiated, the Topopah Spring Member (composed predominantly of welded tuff) of the Paintbrush Tuff was not yet identified as the most suitable geologic unit in which to locate a high-level nuclear waste repository.

Table 1. Compositions of Eight Preliminary Cementitious Mixtures

Component[a]	Expansive Mixtures				Nonexpansive Mixtures			
	81-05[b] (M)[c]	82-22 (M)	82-31 (M)	82-30 (g)	82-19 (M)	82-20 (M)	82-21 (M)	82-24 (g)
Type K cement	--	33.8	33.7	--	--	--	--	--
Class H cement	36.3[l]	--	--	47.3	34.4	21.2	20.5	54.9
E-22 water[d]	--	--	--	20.3	--	--	--	--
Deionized water[e]	16.6	15.9	15.8	--	14.9	9.55	11.3	19.8
Slag,[f] B19	8.29	--	--	--	--	--	--	--
Silica fume,[f] B31	8.34	--	--	--	--	--	--	--
Silica fume,[f] B27	--	7.29	7.25	--	7.58	--	--	12.1
Silica fume,[f] B59	--	--	--	4.75	--	--	--	--
Silica fume,[f] B58	--	--	--	--	--	2.89	3.32	--
Fly ash (low calcium),[f] B25	--	8.18	8.14	--	7.58	--	--	--
Fly ash (high calcium),[f] B62	--	--	--	15.2	--	--	--	--
Silica flour (5 micron),[f] B60	--	--	--	4.82	--	10.3	9.98	12.1
Sand (ASTM C 109)[g]	27.2	33.8	--	--	34.7	55.7	--	--
Granite sand[g]	--	--	33.7	--	--	--	53.9	--
Hemihydrate (Gypseal)[h]	2.22	--	--	6.48	--	--	--	--
Dispersant--Mighty 150[h]	1.15	1.00	1.48	--	0.89	--	--	1.11
Dispersant--Dowell D65[h]	--	--	--	1.12	--	0.41	1.00	--
Defoamer--Dowell D47[h]	--	0.005	0.005	0.02	--	0.005	0.005	--
w/c[i]	0.46	0.47	0.47	0.43	0.43	0.45	0.45	0.36
w/rs[j]	0.30	0.32	0.32	0.28	0.30	0.25	0.25	0.30
In curing solution[k]	E-05	E-25	E-25	E-25	E-25	E-22	E-25	E-25

a. Values for each component are reported as weight percentage of the total mixture.
b. Identification numbers for specific mixtures. The first number indicates the year when the mixture was first designed and the second number represents a unique sample mixture number for that given year.
c. (M) = mortar; (g) = grout.
d. Mixing water; Appendix A gives composition.
e. Mixing water.
f. Silica additives.
g. Aggregate.
h. Admixtures.
i. Water-to-cement ratio.
j. Water-to-reactive-solids ratio.
k. Sample is immersed in specified solution.
l. H-07 cement was used in this mixture, all other class H cements used H-08.

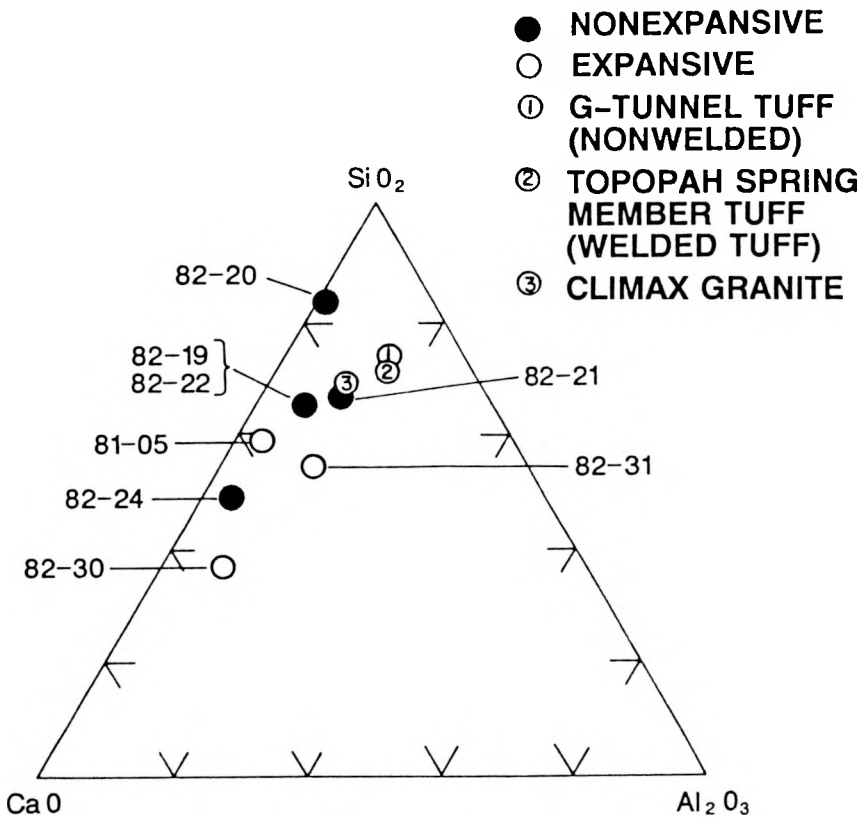

Figure 1. Chemical Compositions of the Eight Preliminary Mixtures and G-Tunnel Tuff, Topopah Spring Member Tuff, and Climax Granite

ratios (w/c). Slow reaction rate is desirable for use in massive pours where heat generation could lead to development of excessive stress buildup. Class H cements have been used extensively for many years, particulary for remote placement, in environments of high ambient temperatures, e.g., deep wells. The expansive property for Mixes 81-05, 82-30, 82-22, and 82-31 was achieved in two ways, both based on the development of ettringite (hexacalcium aluminate trisulfate hydrate). For Mixes 81-05 and 82-30, hemihydrate (Gypseal) was added to the mix. For Mixes 82-22 and 82-31, a Type K shrinkage compensating cement (Chem Comp) was used. In the latter, the expansive agent, calcium sulfoaluminate, is an integral part of the cement in small quantities (2-3%). In both cases, the long-term objective is to prevent a negative volume change as a result of shrinkage of the mass. Maintaining a slight positive stress at the rock/seal interface can reduce the permeability at this interface.

Where fine aggregate is specified for the mortars, either high-purity silica sand graded to ASTM C 109-80 and ASTM C 778-80a (ASTM, 1985a, 1985c) specifications or a granite-based sand graded to the same specifications was used. The granitic sand was derived from the Climax Stock, an intrusive igneous body located at the Nevada Test Site (NTS), and has a bulk composition similar to many welded tuffs of the region (Figure 1). Use of

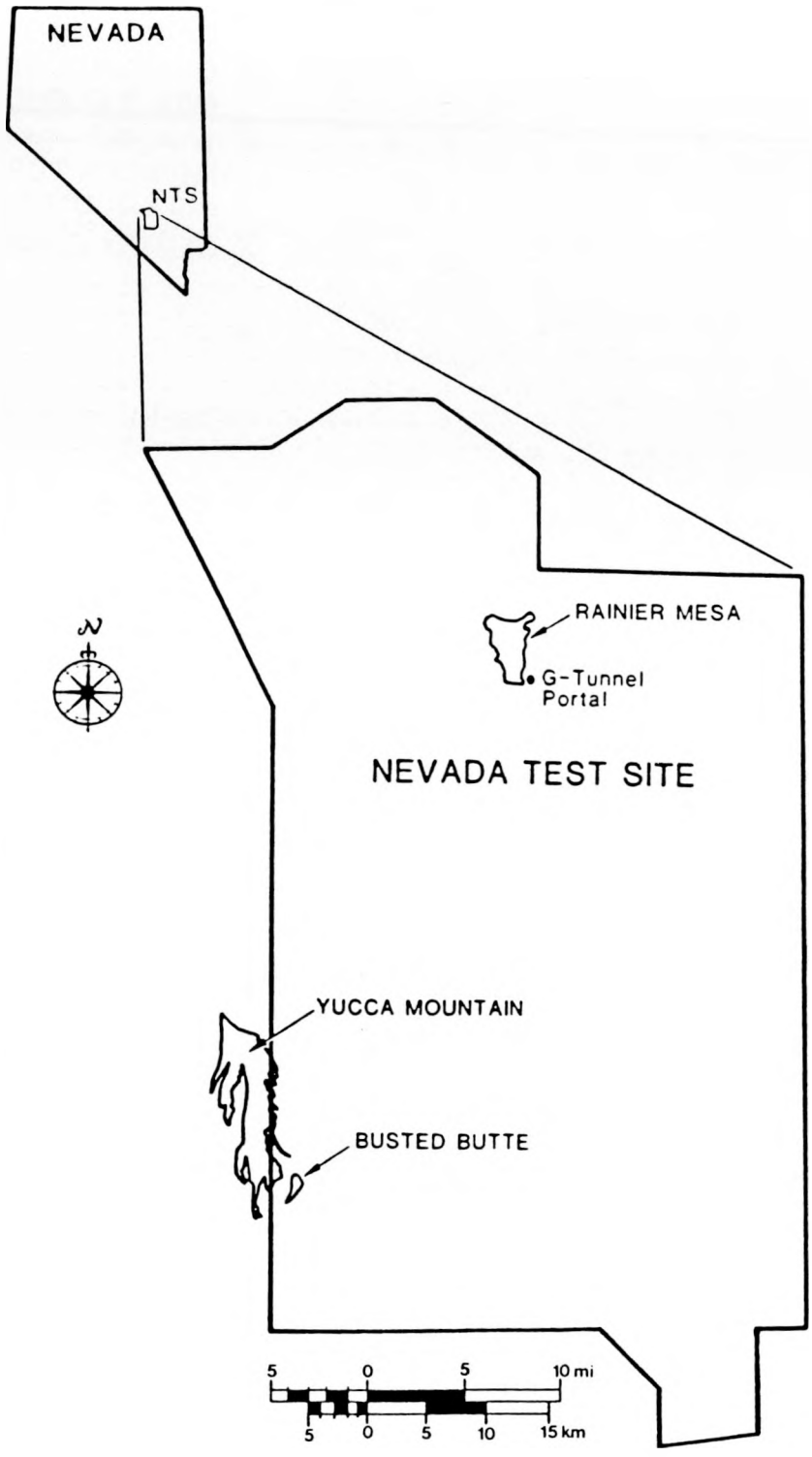

Figure 2. Location Map Showing Busted Butte, G-Tunnel, and Yucca Mountain

this aggregate provided the potential of forming a dense composite material based on an aggregate indigenous to the general area.

All mixes contained various proportions of a fine siliceous component, e.g., fly ash, silica fume, slag, silica flour. There is considerable evidence that the adjustment of composition of the Portland cement matrix of concrete materials to higher silica contents more closely matching the composition of the host rock is a means of generating greater stability and probable long-term durability in repository seal materials (Roy et al., 1979; Roy, 1980; Sarkar et al., 1980). In Portland-cement-based materials, silicates are present, of which tricalcium silicate, Ca_3SiO_5 (abbreviated C_3S)* is the prevalent compound in most cements. Hydration at normal temperatures generally produces a poorly crystalline calcium silicate hydrate, C-S-H,** along with ample calcium hydroxide [$Ca(OH)_2$], the latter being generally the weaker component of the hydrated matrix. The addition of excess silica (which has differing reactivity depending on the nature of the material and curing temperature) may consume $Ca(OH)_2$ as it is liberated from C_3S hydration in the mixture, through a reaction expressed schematically as follows:

$$C_3S + 3H \rightarrow C\text{-}S\text{-}H + 2CH \quad (1)$$

$$CH + S \rightarrow C\text{-}S\text{-}H \quad (2)$$

Reaction 2 is highly favored thermodynamically; i.e., the C-S-H is more stable than calcium hydroxide plus silica (CH + S).

The three types of water used in mixing and curing in Phase I tests are designated as E-01 (deionized water), E-22, and E-25. Waters designated as E-22 and E-25 were selected as part of Phase I, i.e., short-term testing presented in this report. Water designated as E-22 was intended to represent a water having a pH greater than E-25. Water designated as E-25 was intended to represent a water found in a tuffaceous environment. E-25 is based on the composition of waters from Well 73-66 as reported by Winograd and Thordarson (1975, p. C107). Well 73-66 is located approximately 30 km east of Yucca Mountain. Compositions of these waters are presented in Appendix A.

The composition of J-13, which has been accepted more recently as a site-specific standard, is presented for comparison. J-13 water was used as the curing water for formulations developed as a part of Phase II (long-term testing) of this work.

---

*Cement notation: C = CaO, S = SiO_2, H = H_2O, A = Al_2O_3, etc.

**C-S-H (calcium silicate hydrate) has variable C to S ratios depending on temperature: possibly a precursor of tobermorite or other crystalline calcium silicate hydrates.

3.0 PROPERTIES OF THE PRELIMINARY MIXTURES (PHASE I)

3.1 Mineral Phase Assemblages of Cured Samples

At various test intervals, the hydrating mortars and grouts were analyzed by x-ray diffraction. In this manner it is possible to follow the progressive development of ettringite in expansive mixtures and to monitor qualitatively the hydration of all cement phases. Unhydrated cement phases, particularly Ca_2SiO_4(C_2S) and Ca_3SiO_5(C_3S) remain in all samples, along with the major hydration product, poorly crystallized calcium silicate hydrates (C-S-H). Ettringite was readily recognized in cured samples from all expansive formulations. With the maximum curing temperature for these experiments at 60°C, ettringite remained a stable phase.

X-ray diffractograms of cured samples of the mortars were dominated by the mineral(s) of their component sands. Quartz was the dominant phase in mixtures containing silica sand. Quartz, biotite, and feldspars dominated patterns from granitic-sand mixes, and occasionally, chlorite was detected. Minerals identified by x-ray diffraction (XRD) in samples of nonexpansive mixtures are listed in Table 2. Table 3 shows the comparable data for expansive mixtures.

3.2 Rheological Properties

Early stage rheological properties are an important aspect of formulation because the final properties of a structural component, e.g., borehole plug or shaft seal, can be influenced if the grout/mortar/concrete workability is inconsistent with its emplacement mode. Excessive segregation, bleeding, air entrainment, honeycombing, blowholes, etc., may result, altering the integrity and long-term stability of the seal.

Factors influencing rheology include the initial water-to-reactive solids (w/rs) ratio, composition, shape, and size distribution of the aggregate. Dispersing agents are added to the mix in moderation to create the desired flow and to set retardation properties.

Generally, a guideline of up to 3 hr is specified for workability for the mortars and grout and a limit of apparent viscosity is set at <2000 cP at a 150 rpm shear rate after 30 min of mixing. Apparent viscosities for various formulations, measured after 30 min at a shear rate of 150 rpm, are presented in Table 4.

A comparison was made between the mixtures using Class H cement and those using Type K cement, which was designed to compensate chemically for shrinkage (Mixes 82-22 and 82-31). The rheological behaviors of the mixtures are similar; however, as might be expected from the smaller particle size of the Type K cement, the viscosities are greater except for Mix 82-20, which had >55% sand. As other studies have shown (Nakagawa et al., 1982; White and Roy, 1982), the type of sand within the mixture is a critical determinant of rheology.

Table 2. Phases Present in Nonexpansive Mixtures, as Determined by X-Ray Diffraction

Curing Time (days)	Curing Temperature (°C) 38	60
	82-21	
3	quartz	
	oligoclase	
7	biotite	
	chlorite	
28	unhydrated cement*	
	82-19	
3	quartz	
7	unhydrated cement	
14	C-S-H	
28		
	82-20	
7	quartz	
14	unhydrated cement	
28	C-S-H	

*C_3S, C_2S, C_4AF.

Table 3. Phases Present in Expansive Mixtures, as Determined by X-Ray Diffraction

Curing Time (days)	Curing Temperature (°C) 38	60
	81-05	
7	quartz portlandite ettringite	
14	C-S-H unhydrated cement	quartz C-S-H unhydrated cement ettringite
28	quartz ettringite C-S-H unhydrated cement	
	82-22	
3 7 28	quartz ettringite unhydrated cement C-S-H	
	82-31	
3 7 28	oligoclase quartz biotite ettringite chlorite C-S-H unhydrated cement	
	82-30	
3 7 28	quartz ettringite C-S-H unhydrated cement	

Table 4. Apparent Viscosities

Mixture	Apparent Viscosity (cP) (150 rpm after 30 min)
81-05(M)	585
82-22(M)	1,550
82-31(M)	1,785
82-30(g)	1,000
82-19(M)	1,070
82-20(M)	26,900 (at 16 rpm)
82-21(M)	not measured
82-24(g)	not measured

(M) = mortar; (g) = grout.

3.3 Compressive Strength

Unconfined compressive strengths of nonexpansive mortar formulations are given in Table 5. Table 6 shows strength values for expansive mortars and the 82-30 mix grout. These unconfined compressive strengths were determined using ASTM C 109-84 (ASTM, 1985a). In all cases, 2 x 2 in. cubes were tested. According to ASTM C 109, samples were removed from their mold approximately 24 hr after being placed in their mold and then stored in water until testing.

The nonexpansive mortars (Mixtures 82-19, 82-20, and 82-21) developed high early strength, exceeding 39 MPa after 3 days of curing at 38 or 60°C. Expansive samples cured at 38°C showed an increase in strength with longer curing time. However, under the curing conditions of 60°C samples of expansive mixtures achieved an apparent maximum strength by 7 days, followed by a regression in strength of 15-20% by the 28th day of curing. Similar behavior has been observed by Grutzeck et al. (1981) who attributed such a decrease to microfractures induced by expansive stresses in an unrestrained environment. Such strength decreases would probably not be seen in the restrained conditions of subsurface curing within continuous rock strata. For all mixtures, compressive strength was higher at 7 and 14 days of curing at 60°C than it was at 38 or 27°C, reflecting the effect of temperature on hydration.

Compressive strength values were also compared in relation to the type of sand in the mortars. Two of the nonexpansive mixtures (82-20 and 82-21) were identical except for the difference of silica versus granite sand. At 38°C, samples of the nonexpansive mixture with silica sand (82-20) developed strength more rapidly than did those of the comparable granite-sand formulation. The mix with silica sand (82-20) continued to develop greater strength, achieving nearly 100 MPa by 28 days of curing. At 28 days of curing, the strength of the 82-20 mixture is approximately 75% greater than the strength for the 82-21 mixture. Samples of the granitic mixture

Table 5. Unconfined Compressive Strengths (MPa) of Nonexpansive Mortars

Curing Time (days)	Curing Temperature (°C) 38			60		
	82-19	82-20	82-21[a]	82-19	82-20	82-21[a]
3	47.3(1)[b]	--	39.1(3) [1.45]	77.7(3) [3.45]	--	58.4(3) [3.30]
7	74.8(3) [4.05]	51.5(1)	52.3(3) [1.01]	78.1(3) [4.41]	67.2(1)	71.2(2) [1.20]
14	92.4(3) [1.69]	69.2(1)	--	103.4(1)	74.1(1)	--
28	92.0(1)	96.7(2) [0.59]	55.2(3) [2.79]	78.2(2) [14.1]	113.9(2) [0.29]	73.0(3) [1.72]

a. Similar to the 82-20 mixture but with granitic sand instead of silica sand.
b. Number of samples tested in ( ); one standard deviation, 1σ, in [ ].

Table 6. Unconfined Compressive Strengths (MPa) of Expansive Mortars and Grout

Curing Time (days)	Curing Temperature (°C) 38				60			
	81-05[a] (M)[b]	82-30 (g)	82-22 (M)	82-31 (M)	81-05[a] (M)	82-30 (g)	82-22 (M)	82-31 (M)
3	--	92.8(3) [3.07]	78.5(3) [3.36]	67.(3) [0.87]	--	--	114.9(2) [0.0]	97.8(3) [8.82]
7	74.9(5)[c] [5.23]	99.1(3) [3.68]	77.5(1) [--]	88.(3) [6.14]	117.(5) [8.16]	--	118.2(1) [--]	110.9(2) [9.48]
14	85.7(4) [5.12]	--	--	--	87.6(1) [--]	--	--	--
28	87.1(4) [5.43]	98.1(3) [1.74]	96.7(2) [10.96]	113.5(2) [1.75]	98.5(2) [5.96]	--	110.7(2) [3.39]	89.9(1) [--]

a. Cured at 27°C.
b. (M) = mortar; (g) = grout.
c. Number of samples tested in ( ); one standard deviation, 1σ, in [ ].

(82-21) reached their maximum strength, for the time period tested, at 28 days, but experienced an increase in strength of <10% between 7 and 28 days. A similar trend was observed for samples cured at 60°C. The compressive strength of Mixture 82-20 was approximately 55% greater than the compressive strength of Mixture 82-21 at 28 days of curing.

In comparing the effect of fine aggregate between the expansive mixtures, 82-22 and 82-31, the trend in strength development relative to type of sand was reversed for a curing temperature of 38°C, i.e., the expansive mixture containing granite sand achieved higher strengths at both curing temperatures than did its counterpart with silica sand. Cured at 60°C, both of these expansive mixtures achieved extraordinarily high early strength, between 90 and 100 MPa at three days. The difference in strength attributable to the type of sand is less for expansive mixtures (Table 6) than was observed for the nonexpansive mixtures.

3.4 Bulk Density/Porosity

Dry bulk densities of cured samples of mortars typically parallel the relatively high values for compressive strength. The mortars exhibited bulk densities ranging from 1.9-2.2 g/cm^3 (Table 7). For comparison, dry bulk density for the Topopah Spring welded unit is approximately 2.22 g/cm^3, whereas a nonwelded zeolitized unit such as the tuffaceous beds of Calico Hills is about 1.58-1.87 g/cm^3. In general, the densities of the expansive mixtures are lower than those of the nonexpansive mixtures. The presence of ettringite, the hydrated cement phase causing expansion in the expansive mixtures, is suggested as the factor contributing to the lower densities. Development of a lower density can occur as a result of the expansion of the sample in unrestrained environment, i.e., the sample volume increases resulting in lower density. A lower density could also be explained by the fact that ettringite has a lower density, 1.73 g/cm^3 (Lea, 1971, p. 223), than the bulk density of a sample in which ettringite does not develop. Porosities of the expansive mixtures are generally higher than the porosities of the nonexpansive mixtures. These data are consistent with the bulk densities measured for all mortar mixtures (Table 7). The densities and porosities were determined using ASTM C 642-82 (ASTM, 1985e).

3.5 Thermal Conductivity

Thermal conductivities were measured for samples of three nonexpansive mixtures cured at 38 and 60°C, including the 82-20 and 82-21 mixtures for contrasting the effects of two types of sand. All thermal conductivities are relatively high, exceeding the conductivity of dry, nonwelded tuff (usually <1.45 W/mK) or dry, welded tuff (~1.4 W/mK). Thermal conductivity values measured for Mixtures 82-19, 82-20, and 82-21 are listed in Table 8. Because of the greater thermal conductivity of quartzite relative to granite, samples containing silica (quartzitic) sand have higher conductivities than do their counterparts with granitic sand. To illustrate this point, the thermal conductivities for quartzite and granite are approximately 6.7 and 3.2 W/mK, respectively (GSA, 1966, pp. 461-462).

Expansive mixtures exhibited lower thermal conductivities than did the nonexpansive ones, regardless of sand type or curing conditions (Table 9).

Table 7. Dry Bulk Density (g/cc)/Porosity of Nonexpansive and Expansive Mortars[a]

Curing Time (days)	Curing Temperature (°C) 38			60
	82-19	82-20	82-21	82-21
	Nonexpansive			
3	1.93/.16	2.21/.08	1.99/.15	2.04/.14
7	1.96/.16	2.18/.13	1.95/.15	2.00/.14
14	1.94/.19	2.21/.08	--	--
28	1.93/.19	2.22/.07	1.96/.16	2.01/.14

	81-05[b]	82-22	82-31	81-05	82-22	82-31
	Expansive					
3	---	1.98/.18	1.92/.17	---	1.98/.18	1.92/.17
7	1.96/.20	1.96/.18	1.92/.18	2.01/.19	1.99/.15	1.93/.19
14	1.99/.21	---	---	2.01/.17	---	---
28	1.92/.29	1.91/.21	1.92/.19	1.92/.27	1.93/.20	1.94/.19

a. Data based on one sample per test period.
b. Cured at 27°C.

Table 8. Thermal Conductivity (W/mK) of Cured Samples of Nonexpansive Mortars

Curing Time (days)	Curing Temperature (°C) 38			60		
	82-19	82-20	82-21	82-19	82-20	82-21
3	2.95	3.73	2.96	2.69	3.74	2.92
7	2.89	3.56	--	3.04	3.61	--
28	2.66	3.81	3.18	3.16	3.71	2.92

Table 9. Thermal Conductivity (W/mK) of Cured Samples of Expansive Mortars

Curing Time (days)	Curing Temperature (°C)			
	38		60	
	82-22	82-31	82-22	82-31
7	2.96	2.36	3.06	2.33
28	2.08	1.70	2.94	1.89

Thermal conductivities for these mixtures are greater at shorter curing times, possibly related to the development of microcracks in an unrestrained condition. The lower thermal conductivities measured for the expansive mixtures, as compared to the nonexpansive mixtures, is consistent with the lower densities (Section 3.4) for the expansive mixtures. Typically, the higher the density the higher the thermal conductivity (Lea, 1971, p. 588).

3.6 Dimensional Stability

Grout Mixture 82-30 was designed to be expansive. Its linear dimensional change was monitored at 38°C, at both atmospheric pressure (0.1 MPa) and 11 MPa, yielding the data plotted in Figures 3 and 4. Details of how the dimensional stability is measured are given in Appendix B-1. At one atmosphere, the mixture experienced shrinkage or settling during the first 9 hr after mixing, with a length decrease of 0.07%. After this initial change, the grout expanded ~0.04%, recovering approximately 90% of the loss, as shown in Figure 3, in about 30 hr postmixing time. As shown in Figure 4, however, applying a modest pressure of 11 MPa eliminates the initial "apparent" shrinkage. The grout was observed to expand during the entire duration of the test, achieving a change in length of 0.12% after 30 hr.

3.7 Permeability

Water permeabilities of four of the experimental grouts were measured, using the procedure described in Appendix B-4, to determine their capacity to impede water movement. With only two exceptions, the samples have permeabilities $<10^{-8}$ Darcy, which relates to the lowest detectable flow limits of the testing apparatus. These data are summarized in Table 10.

3.8 Interface Permeability

An important factor in repository sealing systems may be the establishment of an adequate bond between the seal material and the host rock. Coincident with good interface bonding is usually a low interface permeability, which can reduce fluid migration through the seal system and potential

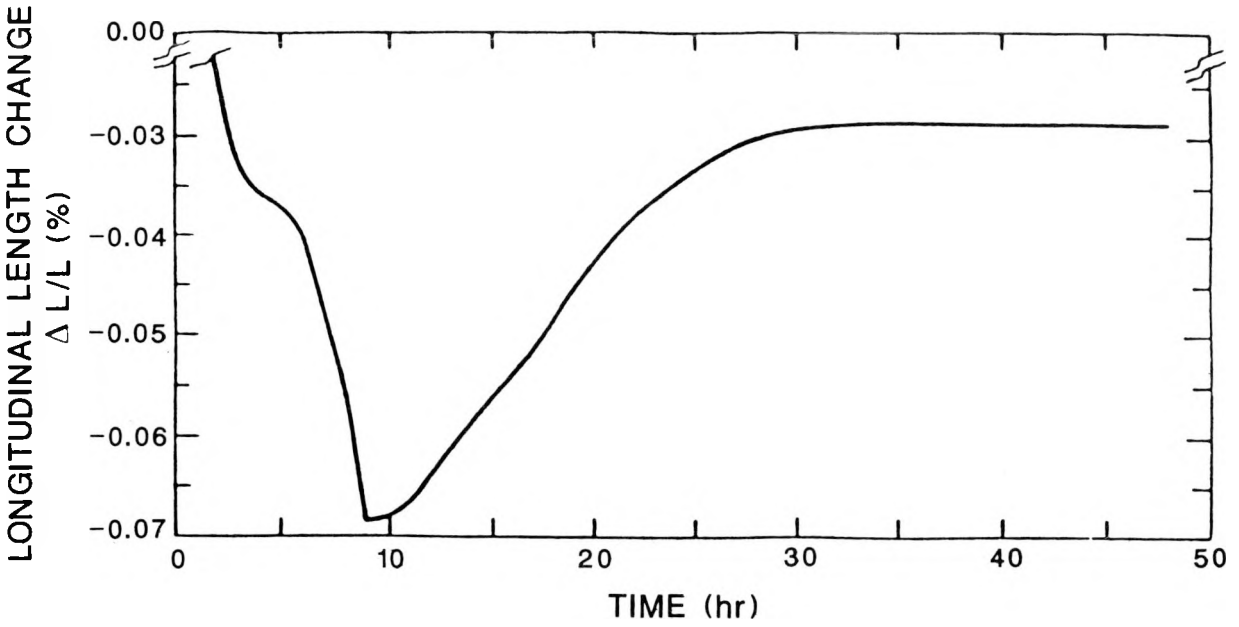

Figure 3. Uniaxial Length Change of a Radially Restrained Sample of Mixture 82-30 (Test Conditions: 38°C and 0.1 MPa)

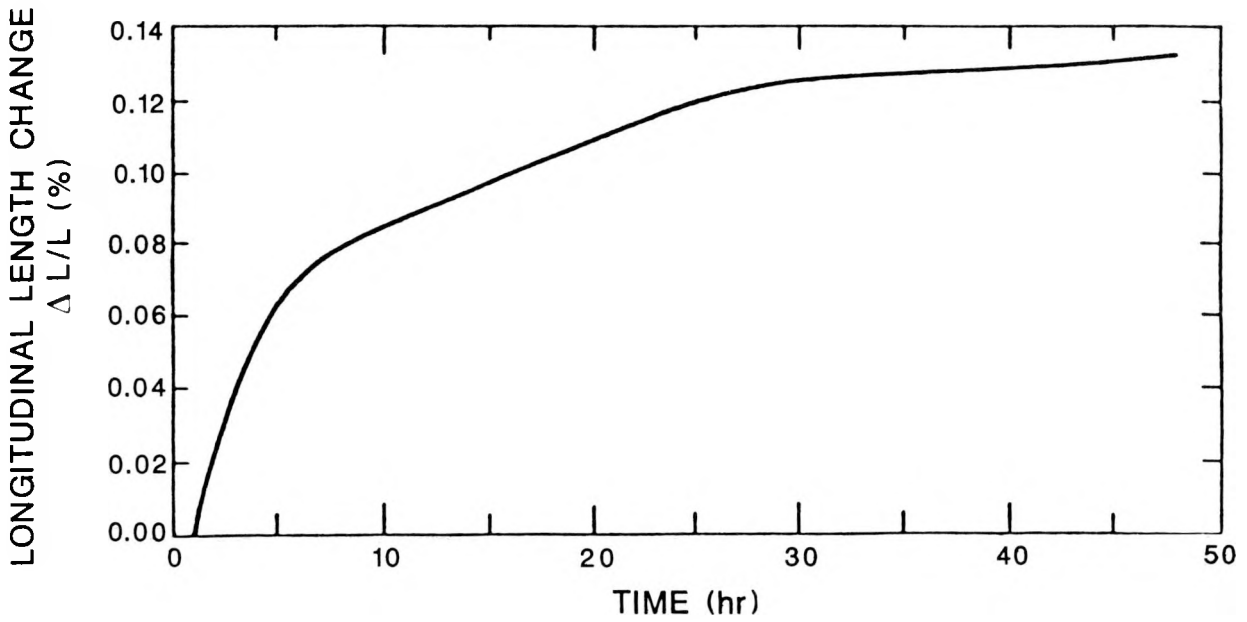

Figure 4. Uniaxial Length Change of a Radially Restrained Sample of Mixture 82-30 (Test Conditions: 38°C and 11 MPa)

Table 10. Water Permeabilities (Darcy) of Nonexpansive and Expansive Mortars

	Nonexpansive				Expansive			
	Curing Temperature (°C)							
Curing Time (days)	38		60		38		60	
	82-19	82-20	82-19	82-20	82-22	82-31	82-22	82-31
7	$<10^{-8}$	1.9×10^{-7}	$<10^{-8}$	$<10^{-8}$	$<10^{-8}$	$<10^{-8}$	$<10^{-8}$	$<10^{-8}$
14	$<10^{-8}$	$<10^{-8}$	$<10^{-8}$	$<10^{-8}$	--	--	--	--
28	$<10^{-8}$	$<10^{-8}$	$<10^{-8}$	$<10^{-8}$	$<10^{-8}$	$<10^{-8}$	$<10^{-8}$	5.5×10^{-7}

Data from one sample per test period.

dissolution at the interface. Where the use of concrete is anticipated, a good bond between the cementitious matrix and the coarse aggregate would be desirable.

The tuff used in preliminary interface experiments was material excavated from nonwelded portions of the Grouse Canyon Member in G-Tunnel in the NTS. The tuff was taken from the excavation of the rock mechanic drift (Zimmerman and Vollendorf, 1982, p. 10). The primary purpose in conducting Phase I interface permeability testing was the result of availability of nonwelded tuff. Furthermore, a comparison of the interfacial permeabilities is only made between the other grout mixtures tested during Phase I testing and the two types of tuff, C48 and C48x (Table 13). Performance of cementitious materials to other rock types should be evaluated independently as done in the Phase II testing with welded tuff. Therefore, because the interfacial permeability testing for Phase I testing was performed with nonwelded tuff and the number of tests are limited, no direct correlation is made between these results and the results from Phase II Testing. Phase compositions of samples of these tuffs were determined by XRD. The major crystalline phases identified by XRD are clinoptilolite and sanidine. Both quartz and a plagioclase feldspar were identified in subordinate amounts (Table 11). The chemical compositions of this and other tuffs used in preliminary and long-term experiments are given in Appendix A.

Bulk density and porosity, using ASTM C 215-85 (ASTM, 1985d), were determined for duplicate tuff samples of different particle size ranges. The mean, dry bulk density was 1.83 g/cm^3 with a porosity of 0.23. For comparison, mean porosity values of 0.12 have been reported for the Topopah Spring welded unit (TSw2), 0.42 for the upper Paintbrush nonwelded unit, which is above the Topopah Spring Member unit, and 0.36 for the tuffaceous

Table 11. Phases Identified in G-Tunnel Tuff by X-Ray Diffraction (C48 and C48x)

Mineral	Composition
clinoptilolite	$(Na,K,Ca,Mg,Fe)_6(Si,Al)_{38}O_{72}\cdot 20H_2O$
sanidine	$(K,Na)AlSi_3O_8$
plagioclase	$(Na,Ca)(Si,Al)_4O_8$
quartz	SiO_2

beds of Calico Hills (zeolitic portion, CHnlz). Water permeability of tuff samples C48 and C48x are reported in Table 12.

The method for preparing samples and determining the permeability between grout or mortar and rock is described by Wakeley and Roy (1982). Briefly, a half-cylinder of tuff is sealed in a metal sleeve sized appropriately for the permeability testing apparatus (in this case, 2.5 cm in diameter and 1.25 cm long). The other half of this cylinder is then filled with the grout being studied. The interfacial region between rock and cement is parallel to the flow path. Measured permeabilities for these samples at up to 28 days of curing are reported in Table 13.

Table 12. Water Permeabilities (Darcy) of Tuffs from G-Tunnel

PSU Code	Permeability, Darcy*
C48	8.7×10^{-7}
C48x	1.05×10^{-7}

*Average of two samples.

All composite samples were examined by binocular microscope, before and after testing, for evidence of separation at the interface or along the restraining sleeve. This examination was performed to provide greater confidence that the interface permeability could be more reliably determined without the contribution of joints in the tuff, mortar, or grout. Further, no separation or cracking of the grout, mortar, or tuff was observed. For Mixes 82-22 and 82-19 in contact with C48 tuff, measured permeability was lower for samples cured at the higher temperature (90°C), regardless of curing time. Mix 82-22 exhibited low permeabilities in contact with C48 tuff and high permeability with C48x tuff. Clearly, these

Table 13. Interfacial Permeability Values Measured for Mortars or Grouts with G-Tunnel Tuff (C48 or C48x)

Mix	Tuff	Permeability (Darcy)	Curing Temperature (°C)	Curing Time (days)
82-21 (M)	C48	1.4×10^{-6}	60	14
		1.8×10^{-6}	90	14
82-22 (M)	C48	2.7×10^{-6}	38	14
		1.2×10^{-6}	60	14
		3.7×10^{-7}	90	14
		4.0×10^{-6}	38	28
		1.2×10^{-6}	60	28
		2.4×10^{-7}	90	28
	C48x	1.6×10^{-4}	38	28
		1.8×10^{-3}	60	28
82-19 (M)	C48	1.2×10^{-4}	60	28
		3.1×10^{-5}	90	28
82-24 (g)	C48	6.5×10^{-5}	60	28
		4.7×10^{-5}	90	28
82-31 (M)	C48	1.8×10^{-6}	60	21

(M) = mortar; (g) = grout.

two similar rocks from related tuff units exhibit different interface properties, even in contact with a mixture that is chemically compatible with both tuffs. The primary reason for the different interface properties is postulated to be the textural differences observed between C48 and C48x tuff. Tuff C48x is more friable than C48. Tuff C48 is also a finer-grained material than Tuff C48x.

3.9 Bond Strength at Interface

A poor bond between cement and aggregate can be a major cause of low strength and poor durability of concrete. Additionally, in a plug/seal application the bond formed between the mortar/grout plug at the interface with the host repository rock can provide a permeable flow path where bonding is inadequate.

Tests were initiated with two of the preliminary mixtures to determine the mechanical strength of the interface bond. The direct tension (Appendix B-3) method was adopted as that which minimizes the effects of peripheral interface flaws. Test samples were prepared using G-Tunnel tuff (nonwelded tuff from the Grouse Canyon Member in G-Tunnel) in conjunction with Mixes 82-19, 82-20, and 82-22. Cylinders 2.54 cm in diameter were cored from the rock and their ends faced perpendicular to the cylinder axis. Test mortar was prepared according to ASTM C 305-82 (ASTM, 1985b) and cast in contact with the tuff cylinder end.

The results of these studies are shown in Figure 5. The preliminary results showed an increase in bond strength with curing time, and provided a technique for later studies (Phase II), which would include the effects of surface treatment using site-specific, welded tuff.

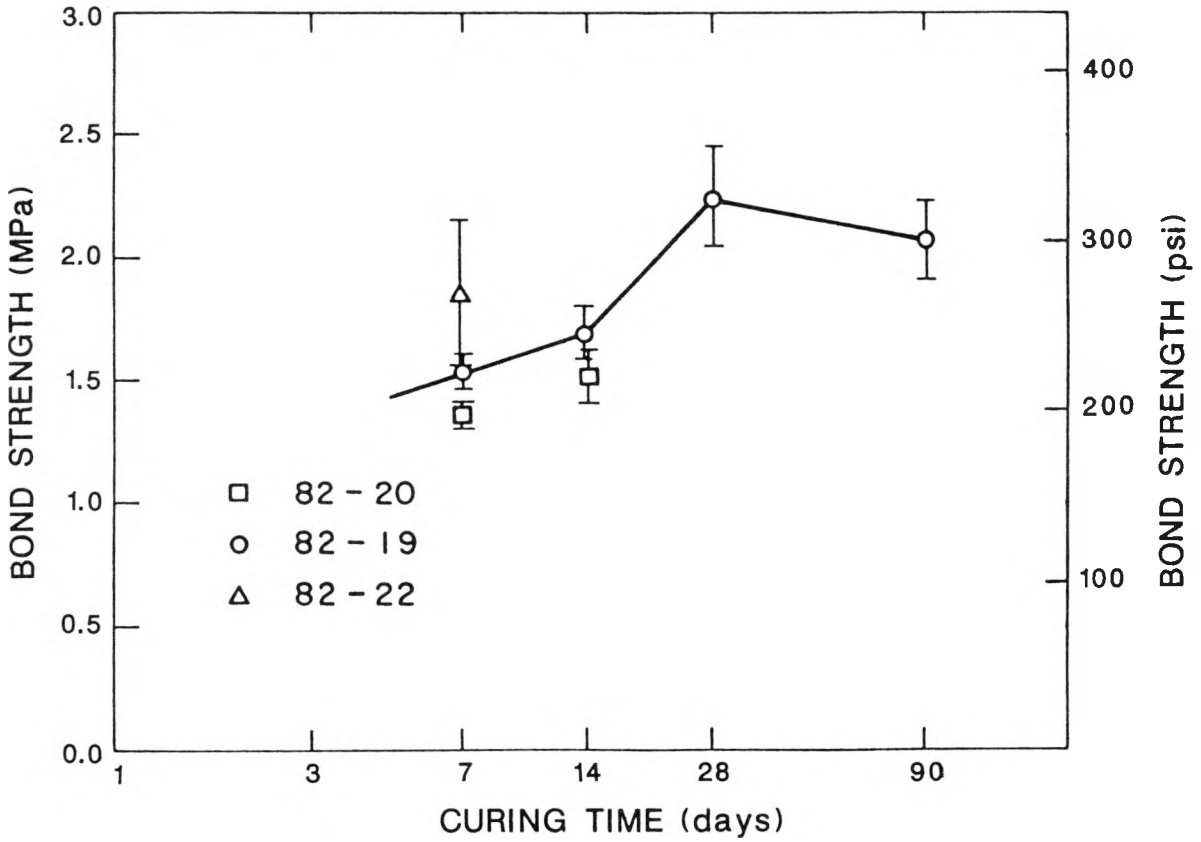

Figure 5. Bond Strength Between Mixtures 82-19, 82-20, 82-22, and G-Tunnel Tuff

4.0 EVALUATION OF PRELIMINARY STUDIES

Properties of virtually all of the preliminary mixtures met or exceeded preliminary selection criteria (i.e., desirable properties) for a cementitious material for use in a tuff repository. These criteria are moderate strength, low matrix permeability, low interface permeability, and adequate workability. To better understand the performance of a potentially usable grout, one mortar and one grout formulation were selected for more detailed testing. Mortar formulation 82-22 was selected for the following reasons. Of all the expansive mortar mixtures, Mixture 82-22 had the highest silica content and was closest to the bulk composition of the nonwelded and welded tuff shown in Figure 1. It is presumed that the closer the bulk chemistry of a material is to its emplacement environment, the lower is the potential for the modification of the material bulk chemistry. Therefore, the potential modification of its physical and mechanical properties will also be lower. In addition to this reason for selecting Mixture 82-22, several other reasons are given below.

The strength development for Mixture 82-22 was good. Of all the expansive mortars, it provided high, unconfined compressive strength for both 60 and 38°C curing temperatures. Although Mixture 82-31 had high strength development at a curing temperature of 38°C, it was significantly lower than the strength of Mixture 82-22 at 60°C, i.e, 89.9 MPa (Mixture 82-31) versus 110.7 MPa (82-22). The unconfined compressive strengths for nonexpansive mixtures were generally lower than those for expansive mixtures. The exception was Mixture 82-20, which had strength development comparable to Mixture 82-22.

The permeabilities were low (generally $<10^{-8}$ Darcy) for all expansive and nonexpansive mixtures while the interface permeability associated with Mixture 82-22 was consistently lower or comparable to the interface permeability associated with the other mixtures tested under similar conditions of curing temperature, curing time, and the same tuff. So, while interface permeability was not necessarily discriminating, the bond exhibited by Mixture 82-22 and subsequently its interface permeability was low.

In addition to the selection of Mortar 82-22 for further testing, Grout 82-30 was also selected because, like Mortar 82-22, it represented a dense, pumpable grout suitable for borehole and fracture/fault sealing. The viscosities of Grout 82-30 and Mortar 82-22 were 1,000 and 1,550 cP, both meeting the guideline of <2,000 cP at 150 rpm shear after 30 min of mixing. While testing of the two grouts was more limited than the testing of the mortars, testing performed on Grout 82-30 did show favorable characteristics. In addition to its positive expansion under confining stress (Figure 4), it showed high unconfined compressive strength after curing 28 days at pressure and temperature conditions of 98.1 MPa (Table 6) and 38°C.

5.0 PROPERTIES OF TWO MIXTURES FROM LONG-TERM STUDIES (PHASE II)

The long-term studies consisted of the following:

1. Continued physical/mechanical testing of two formulations (82-22 and 82-30) under a range of curing conditions which included three curing temperatures (38, 60, and 90°C) for periods up to 2 yr. Unless otherwise noted, the storage conditions of the samples tested under Phase II were the same as in Phase I.

2. Volume stability studies based on longitudinal expansion of radially restrained samples (conducted under saturated vapor conditions) and expansive force measurements in a restrained system using Formulations 82-22 and 82-30.

3. Bond strength determinations and seal/host interface permeability measurements using a site-specific host material (Topopah Spring Member tuff) with Formulations 82-22 and 82-30.

4. The formulation and limited testing of an additional mix (84-12) based on retaining the favorable physical/mechanical properties of 82-22 and 82-30, but modified geochemically to maintain an intermediate pH with reduced sulfate content (84-12) to lessen the potential of sulfate reacting as a complexing agent.

Unless otherwise stated, all mixtures were prepared and tested using the same procedures used in Phase I testing. Test samples of both Formulations 82-22 and 82-30 were cured in E-25 and E-22 water as noted in the Phase I study (Table 1).

5.1 Long-Term Physical/Mechanical Properties of 82-22 Mortar

Unconfined compressive strengths (using ASTM C 109-84; ASTM, 1985a) measured for Mix 82-22 were somewhat erratic, as shown in Table 14.* For samples cured at 38°C, strength increased from 7 to 28 days, dropped sharply by 90 days, and for the data recorded reached a maximum between 90 and 360 days. The compressive strength dropped by 50% from 180 to 360 days, regaining it at 720 days. Samples from 60°C curing showed a similar decrease at 360 days, but curing at 90°C produced less erratic results with curing time, gaining a high strength early and maintaining it through 360 days.**

---

*Samples tested were 2 x 2 in.

**Results from Phase I testing of Formulation 82-22 samples indicate lower unconfined compressive strengths than samples from Phase II testing. The proportions of constituents in 82-22 and the testing conditions were similar for Phases I and II testing. The variations in compressive strength values could be attributable to the number of samples tested, to experimental errors, or to slight variations in preparing and testing Phases I and II samples. These variations suggest the need to consider the factors mentioned above.

Table 14. Unconfined Compressive Strength (MPa) of Mixture 82-22

Curing Time (days)	Curing Temperature (°C) 38	60	90
7	103.31(1)*	--	119.5(3) [8.79]
28	127.6(3) [5.58]	137.3(1)	114.0(3) [3.75]
56	112.6(2) [9.21]	--	113.2(2) [12.42]
90	88.5(2) [6.72]	--	103.4(1)
180	130.95(2) [2.78]	130.71(3) [8.29]	--
360	62.4(2) [8.77]	60.4(2) [2.91]	124.0(1)
720	122.0(1)	--	--

*Number of samples tested in ( ); one standard deviation, 1σ, in [ ].

The dynamic Young's modulus of elasticity measured according to procedures in ASTM C 215 (ASTM, 1985d) was introduced as a nondestructive test for approximating degradation. Although no simple relationship exists between dynamic modulus and compressive strength, correlations do exist when changes in dynamic modulus are produced by internal structural changes and comparisons made of the same formulation as a function of time (Stanton, 1944, pp. 17-20). On this basis it appears to be a good indicator of development of strength as a result of the continuation of hydration of cement and microcrack development.

Dynamic modulus of samples of Mixture 82-22 increases with time at 38 and 60°C, but shows a slight decrease after 92 days of curing at 90°C (Table 15). These samples were cured at high humidity (not immersed), and the fluctuations in modulus at the higher temperatures possibly reflect some drying of the samples which would reduce the amount of available water that could complete hydration. As indicated in Table 15, drying and microcracking of the 82-22 samples, cured for 426 days at 90°C, was noted before dynamic moduli testing. This microcracking would cause the lower dynamic moduli measured for these 82-22 samples. Data available for static modulus* of Mixture 82-22 (Table 16) parallel the trends in compressive strength. Permeability remained low throughout the test period (Table 17).

*Samples used to determine the static Young's modulus were discarded following testing. Samples used to determine the dynamic Young's modulus were not discarded. Following a specific time and temperature condition a sample was tested and then returned to the same storage conditions.

Table 15. Dynamic Young's Modulus (GPa) of Mixture 82-22

Curing Time (days)	Curing Temperature (°C)		
	38	60	90
7	33.0(2)[a] [0.28]	--	--
31	34.1(2) [0.41]	31.8(2) [0.21]	31.6(2) [0.069]
56	34.1(2) [0.34]	32.8(2) [0.14]	31.7(2) [0.069]
92	35.1(2) [0.34]	33.9(2) [0.28]	32.6(2) [0.28]
181	35.4(2) [0.28]	34.1(2) [0.21]	30.5(2) [0.76]
426	35.4(2) [0.28]	34.1(2) [0.28]	22.8(2)[b] [0.28]

a. Number of samples tested in ( ); one standard deviation, 1σ, in [ ].

b. While the measurements of these samples are accurate, the curing conditions of the samples were different from all other 82-22 samples tested for dynamic moduli. It was observed that water in the bottom of the container housing these two samples had evaporated. It was also noted that these two samples had undergone some drying between 181 and 426 days of curing as indicated by the development of microcracks at the surface of the samples. Therefore, this data is invalid.

Dry bulk density and porosity of Mixture 82-22 (Table 18) are generally constant for a given curing temperature. A slight decrease in measured bulk density accompanies the strength drop (and possible microcracking) at 360 days of curing for samples at 38°C, but this is not observed for samples cured at 60°C. After 360 days of curing at 90°C, the compressive strength is high while the bulk density drops. Therefore, the bulk density does not appear to be a good indicator in predicting trends of the unconfined compressive strength for samples cured at slightly elevated curing temperatures.

Table 16. Static Young's Modulus (GPa) of Mixture 82-22

Curing Time (days)	Curing Temperature (°C) 38	60	90
90	5.51(2)* [0.36]	--	6.49(1)
180	9.89(2) [0.23]	8.53(1)	--
360	3.08(1)	2.52(1)	9.00(1)

*Number of samples tested in ( ); one standard deviation, 1σ, in [ ].

Table 17. Water Permeabilities (Darcy) of Mixture 82-22 in Long-Term Experiments[a]

Curing Time (days)	Curing Temperature (°C) 38	60	90
7	$<10^{-8}$[b]	---	$<10^{-8}$
28	$<10^{-8}$	$<10^{-8}$	$<10^{-8}$
56	$<10^{-8}$	---	$<10^{-8}$
90	$<10^{-8}$	---	$<10^{-8}$
180	$<10^{-8}$	$<10^{-8}$	---
360	$<10^{-8}$	$<10^{-8}$	---
720	$<10^{-8}$	---	---

a. Results based on single measurement per test period.
b. $<10^{-8}$ signifies permeability lower than the detection limit.

Table 18. Dry Bulk Density (g/cc)/Porosity of Mixture 82-22*

Curing Time (days)	Curing Temperature (°C)		
	38	60	90
7	1.91/.19	--	1.93/.13
28	1.96/.19	1.93/.19	2.01/.08
56	1.94/.21	--	1.99/.10
90	1.89/.19	--	1.94/.11
180	1.91/.21	1.93/.17	--
360	1.87/.18	1.94/.16	1.87/.15
720	1.94/.20	--	--

*Results based on single measurement.

5.2 Long-Term Physical/Mechanical Properties of 82-30 Grout

Compressive strength of the expansive grout was >100 MPa at 38°C when cured 56 days, showed a marked strength decrease by 360 days, and regained strength again at 2 yr. Samples from 60°C curing maintained their high strength and showed very little strength decrease at the longest curing time. These data appear in Table 19.

Samples cured 180 days at 90°C had low compressive strength values compared to those from other test ages at this temperature, and samples did not break in the expected fashion, i.e., a cone-shaped pattern; rather the sample broke up into many small pieces. Apparent recovery of strength at 360 days in this case was associated with a normal failure pattern, i.e. an "hourglass" failure shape or shear failure of test samples.

Values for static modulus were again generally consistent with the range of compressive strengths (Table 20). Dynamic moduli of samples of 82-30 increased with time except for those cured at 90°C, which decreased after 61 days of curing (Table 21).

Bulk densities are lower for the grout (82-30) than the mortar (82-22) (Tables 18 and 22). The porosities of Mixtures 82-22 and 82-30 decrease with increased curing temperature, but show no obvious trend with time. Again, permeability remained low; it was less than the lower limit of the testing method (10^{-8} Darcy) for up to 360 days of curing at 38°C (Table 23).

Table 19. Unconfined Compressive Strength (MPa) of Mixture 82-30

Curing Time (days)	Curing Temperature (°C)		
	38	60	90
7	93.8(3)* [0.62]	--	107.0(3) [5.22]
14	77.4(2) [0.14]	--	74.9(2) [3.68]
28	92.6(3) [3.05]	114.8(3) [6.29]	109.3(1)
56	119.7(1)	--	128.2(1)
90	115.2(2) [6.72]	--	73.15(2) [1.20]
180	114.8(2) [0.15]	136.6(1)	55.4(1)
360	71.4(3) [1.71]	125.8(3) [8.30]	83.5(3) [5.37]
720	151.1(3) [7.98]	--	106.2(3) [5.46]

*Number of samples tested in ( ); one standard deviation, 1σ, in [ ].

5.3 Longitudinal Expansion of Mixtures 82-22 and 82-30

As previously stated, the early expansion or shrinkage of a mixture can influence the bond between the mixture and the rock. Measurements of length change were carried out for Mixtures 82-22 and 82-30, using the method described in Appendix B-1. All samples that were evaluated for length change were cured in a closed system containing saturated water vapor.

The longitudinal expansion tests for Mixture 82-22 were conducted under three conditions: 38 and 90°C at atmospheric pressure and 38°C at 6.9 MPa. This mixture was formulated as specified in Table 1 with ASTM C 109 sand and duplicated with sand derived from Topopah Spring Member tuff, sieved to the same size fractions. The addition of a Topopah Spring Member tuff was intended to monitor the effect of the mixture containing site-specific fine aggregate. Figure 6 shows uniaxial length change of restrained bars of Mixture 82-22 at different temperatures and pressures, with the results of a tuff-sand test given for comparison. Length change curves for Mixture 82-22, formulated with tuff sand and cured at 38 and 90°C, are compared in Figure 7. The values of 6.9 MPa and 90°C represent upperbound emplacement conditions for grout assumed for the testing program presented in this report.

Table 20. Static Young's Modulus (GPa) of Mixture 82-30

Curing Time (days)	Curing Temperature (°C) 38	60	90
7	7.45(3)* [0.030]	--	7.99(3) [0.33]
14	5.91(1)	--	4.34(3)
56	8.73(1)	--	9.10(1)
90	8.32(2) [0.052]	--	3.28(1)
180	8.27(2)	8.10(1)	--
360	4.68(3) [0.24]	7.88(2) [0.32]	5.43(1)

*Number of samples tested in ( ); one standard deviation, 1σ, in [ ].

Table 21. Dynamic Young's Modulus (GPa) of Mixture 82-30

Curing Time (days)	Curing Temperature (°C) 38	60	90
7	26.4(2)* [0.069]	27.4(2) [0.28]	27.0(2) [0.55]
14	27.5(2) [0.069]	28.2(2) [0.14]	27.6(2) [0.35]
28	27.7(2) [0.14]	28.5(2) [0.069]	27.9(2) [0.41]
61	28.1(2) [0.21]	29.2(2) [0.35]	28.4(2) [0.21]
112	28.7(2) [0.28]	30.1(2) [0.14]	26.4(2) [1.9]
190	29.5(2) [0.069]	30.8(2) [0.14]	20.3(2) [1.6]
446	30.1(2) [0.21]	30.9(2) [0.14]	--

*Number of samples tested in ( ); one standard deviation, 1σ, in [ ].

Table 22. Bulk Density (g/cc)/Porosity of Mixture 82-30*

Curing Time (days)	Curing Temperature (°C)		
	38	60	90
7	1.78/.34	--	1.81/.21
14	1.78/.34	--	1.83/.16
28	1.80/.33	1.82/.29	1.86/.12
56	1.82/.32	--	1.88/.10
90	1.83/.30	--	1.87/.13
180	1.82/.33	1.85/.26	--
360	1.82/.32	1.81/.31	--
720	1.95/.19	--	--

*Results based on single measurement per test period.

Table 23. Water Permeabilities (Darcy) of Mixture 82-30 in Long-Term Experiments

Curing Time (days)	Curing Temperature (°C)		
	38	60	90
7	$<10^{-8}$ [a]	--	4.5×10^{-8}
14	$<10^{-8}$	--	$<10^{-8}$
28	$<10^{-8}$	$<10^{-8}$	2.5×10^{-7}
56	$<10^{-8}$	--	1.6×10^{-4} [b]
90	$<10^{-8}$	--	2.6×10^{-7}
360	$<10^{-8}$	$<10^{-8}$	--
720	6.68×10^{-7}	--	--

a. Where value reported is $<10^{-8}$, permeability was lower than the detection limit of the apparatus as measured.
b. Permeability was determined at 75 days and the permeability was $<10^{-8}$ Darcy. No observable flaws were detected in the sample tested at 56 days.

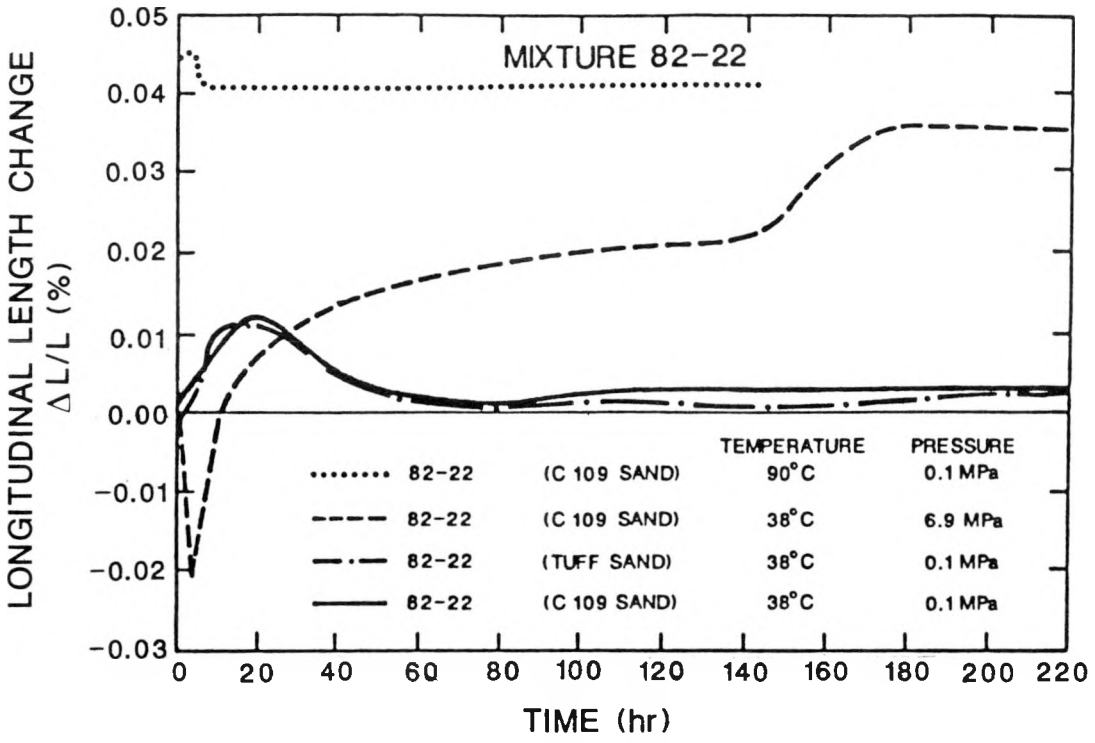

Figure 6. Uniaxial Length Change of Radially Restrained Samples of Mixture 82-22 (Cured at Different Temperatures and Pressures)

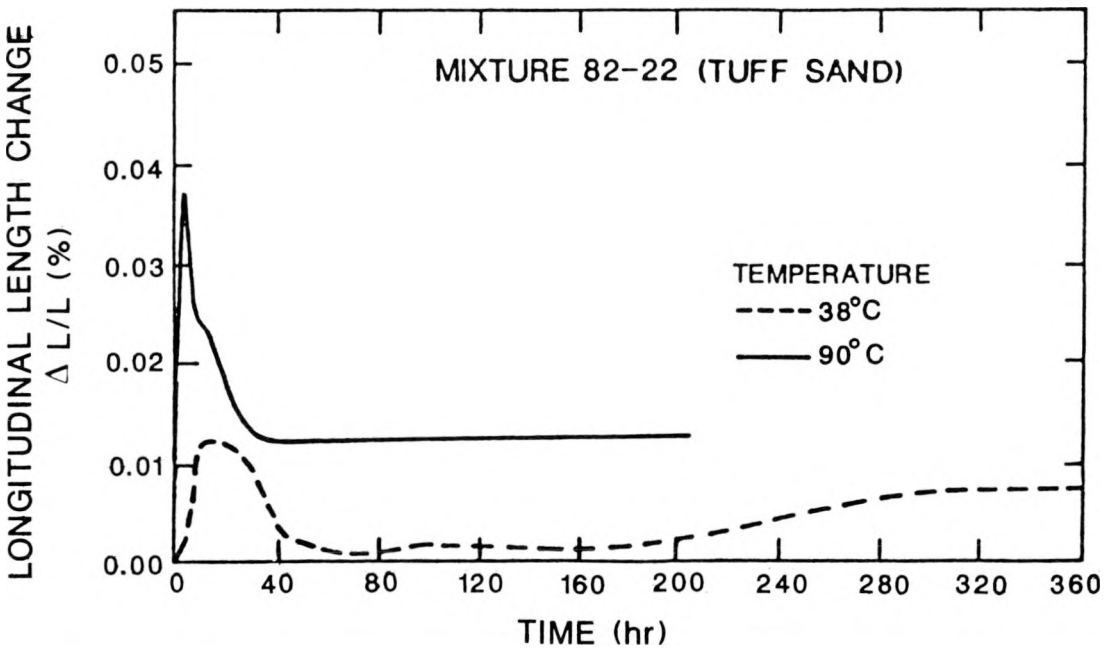

Figure 7. Uniaxial Length Change of Radially Restrained Samples of Mixture 82-22 with Tuff Sand (Cured at Different Temperatures and a Pressure of 0.1 MPa)

Mixture 82-30 was tested at atmospheric pressure at both 38 and 90°C. Figure 8 shows uniaxial length change of Mixture 82-30 at both temperatures.

Curves are characterized by an initial peak that is attributable to expansion of pore water within the hydrating mix. This peak rapidly attenuates, as temperature equilibrium is reached. Subsequently, expansion is initiated gradually while still in a semiplastic state, as the expansive component (ettringite) forms. After a period of time, the grout reaches a steady state beyond which there is no further change in length, provided curing conditions are kept constant.

The final linear length change is given in Table 24. These data show several trends. Mixture 82-22 is less expansive than 82-30, a feature that was expected because of the sand content of 82-22. The expansion of 82-22 formulated with tuff sand is almost two and one-half times greater than that of 82-22 containing C 109 silica sand. Because this tuff does not contain any expansive zeolite minerals, expansion cannot be attributed to the properties of the minerals in the fine tuff aggregate; however, other minerals in the tuff sand may be reactive to the cementitious phases of the 82-22 mixture, resulting in expansion. Results from detailed laboratory analyses were not available to identify the exact mechanism for expansion.

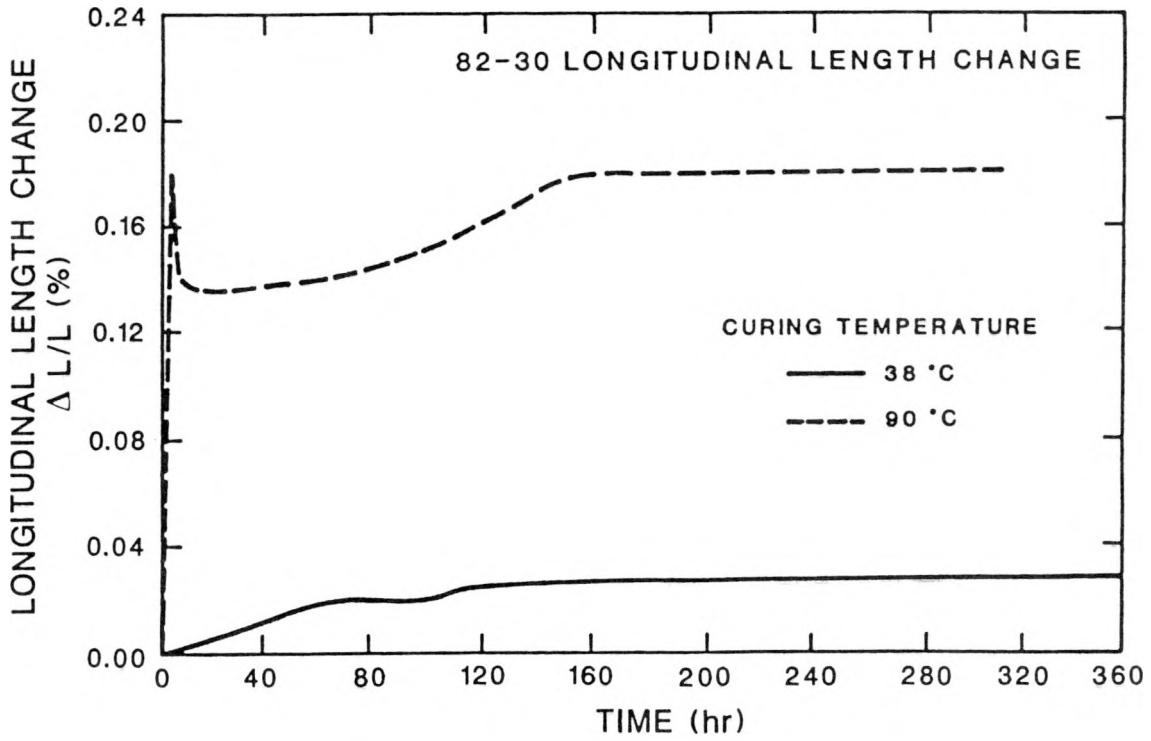

Figure 8. Uniaxial Length Change of Radially Restrained Samples of Mixture 82-30 (Cured at Different Temperatures and a Pressure of 0.1 MPa)

Table 24. Expansive Characteristics of Mixtures 82-22 and 82-30 Under Several Curing Conditions

	Mix 82-22						
	C 109 Sand (0.1 MPa)		C 109 Sand Pressurized (6.9 MPa)	Tuff Sand (0.1 MPa)		Mix 82-30 (0.1 MPa)	
	Curing Temperature (°C)						
	38	90	38	38	90	38	90
Final Length Increase, (ΔL/L, %)	0.0038[a]	0.041	0.056[b]	0.0093[c]	0.012	0.028	0.18
Radial Stress (MPa)	0.50	--	--	0.75	--	2.0	8.6

a. Measured at 38 days.
b. Total, longitudinal length change measured from minimum volume after pressurization.
c. Measured at 34 days.

"Final" expansion of both 82-22 and 82-30 (containing C 109 sand) at 90°C is approximately 6-10 times that experienced by samples of the same mixture at 38°C. Samples cured at 90°C undergo rapid expansion as a result of thermal effects. In addition to the external heat provided by the curing chamber, additional heat is liberated rapidly as hydration of the cement occurs. For samples cured at 90°C, the rate of hydration is faster than that for the samples cured at 38°C (Soroka, 1979, p. 40). Because of this rapid heat evolution and the higher temperature of the curing chamber (90°C), large expansion of the samples occurs immediately. Further, this higher temperature will accelerate the setting time (Barnes, 1983, pp. 497-498), fixing the internal structure of the sample, thereby reducing the contraction of the sample following the initial buildup of heat. Theoretically, greater expansion of the 90°C samples can occur because surface tension of water and subsequently the tension in the capillary water in the unhardened paste is less at higher temperatures. This reduction of internal forces between the free water and the compounds within the paste will result in volumetric expansion of the sample (Soroka, 1979, p. 140).

To illustrate the magnitude of expansion resulting from the higher temperatures in the curing chambers, the following calculation is presented. The change in length of the sample can be defined as follows:

$$\Delta L = L \cdot \alpha \cdot \Delta T \quad ,$$

where

ΔL = change in length of the sample
L = original length of the sample
α = coefficient of thermal expansion
ΔT = difference between the temperatures of the curing chambers.

The values selected are $L = 7.25$ in. (Appendix B-1), $\alpha = 10 \times 10^{-6}$ per °C to 20×10^{-6} per °C for hardened paste (Soroka, 1979, p. 139), and $\Delta T = 52$°C (difference between the 90 and 38°C curing conditions; note that the heat liberated from the hydration of the cement is not included). Using the formula and values above, the computed values for ΔL would be 0.0038 in. (0.0095 cm) and 0.0075 in. (0.019 cm) for the range of α values considered. These ΔL values would correspond to $\Delta L/L$ values of 0.05 and 0.10%. These values illustrate the potential magnitude of thermal expansion for samples cured at higher temperatures.

5.4 Expansive Stress of Mixtures 82-22 and 82-30

In the initial stages of curing, the expansive grout or mortar will generate stress against the borehole or shaft wall, as the volume increases through formation of ettringite or other expansive hydrated phases. The purpose of these experiments was to determine the radial stresses that would be generated by the cementitious mixtures, under restraint simulating that of the tuff host rock in repository conditions.

A series of experiments was designed to determine expansive stress. A description of the apparatus used and derivation of test conditions are given in Appendix B-2.

Figure 9 compares stress measurements for Mixture 82-22 curing at 25 and 38°C for up to 800 hr after initiation of the experiment. Data from this mixture formulated with tuff sand appear in Figure 10. A comparison of 38 and 90°C curing for Mixture 82-30 appears in Figure 11. The two mixtures are contrasted in Figure 12, which shows much greater stress being generated by the 82-30 grout than the 82-22 mortar, in which the sand in the mixture mitigates stress generation. Because sand represents a comparatively inert material, there is a proportionately lesser amount of material that can chemically react and contribute to expansion of the mixture.

All stress curves reveal several stages of expansion. The initial stresses represent a thermal phase, occurring with early heat liberation. These initial thermal stresses are of short duration and have little effect on the ultimate strength of the cementitious materials, because the latter is still in a plastic state when the stresses occur.

The second phase of expansion occurs after the cement reaches its thermal maximum, where rapid cooling causes a drop in measured stress. At least two

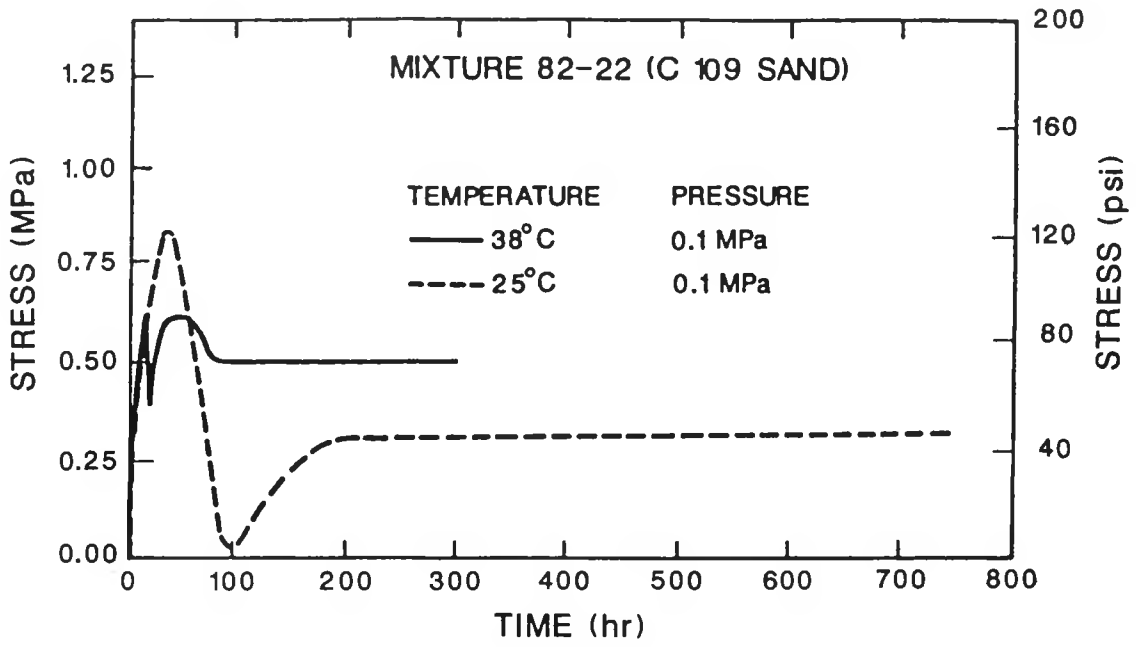

Figure 9. Radial Stresses of Mixture 82-22 (Cured at Different Temperatures and a Pressure of 0.1 MPa)

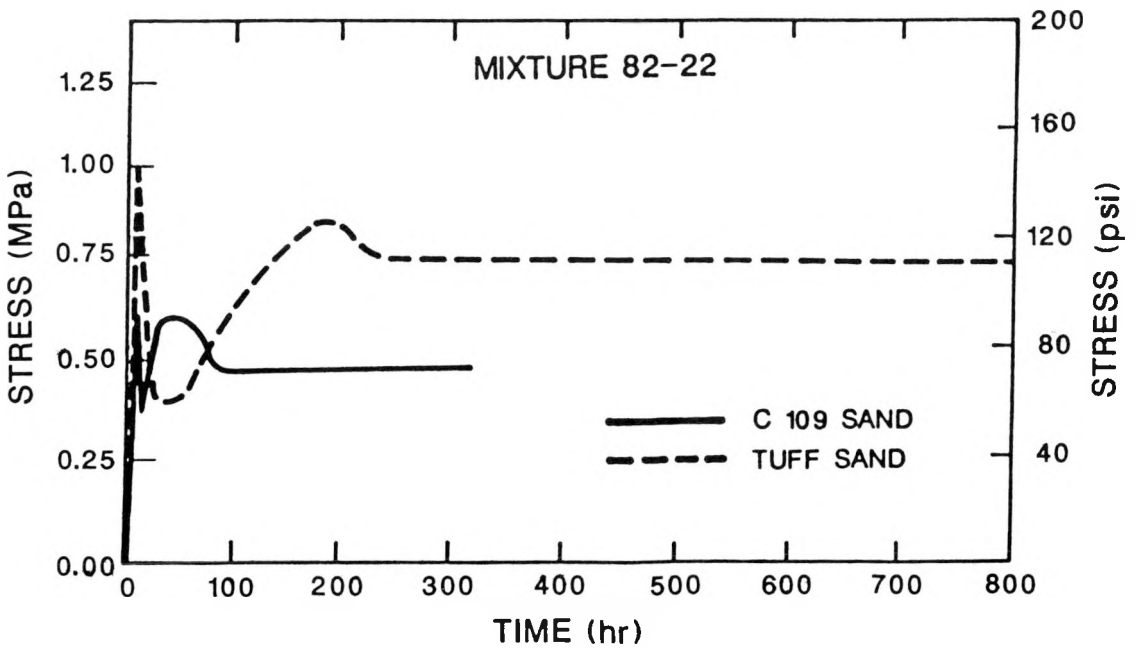

Figure 10. Radial Stresses of Mixture 82-22 Using Different Sands (Cured at 38°C and a Pressure of 0.1 MPa)

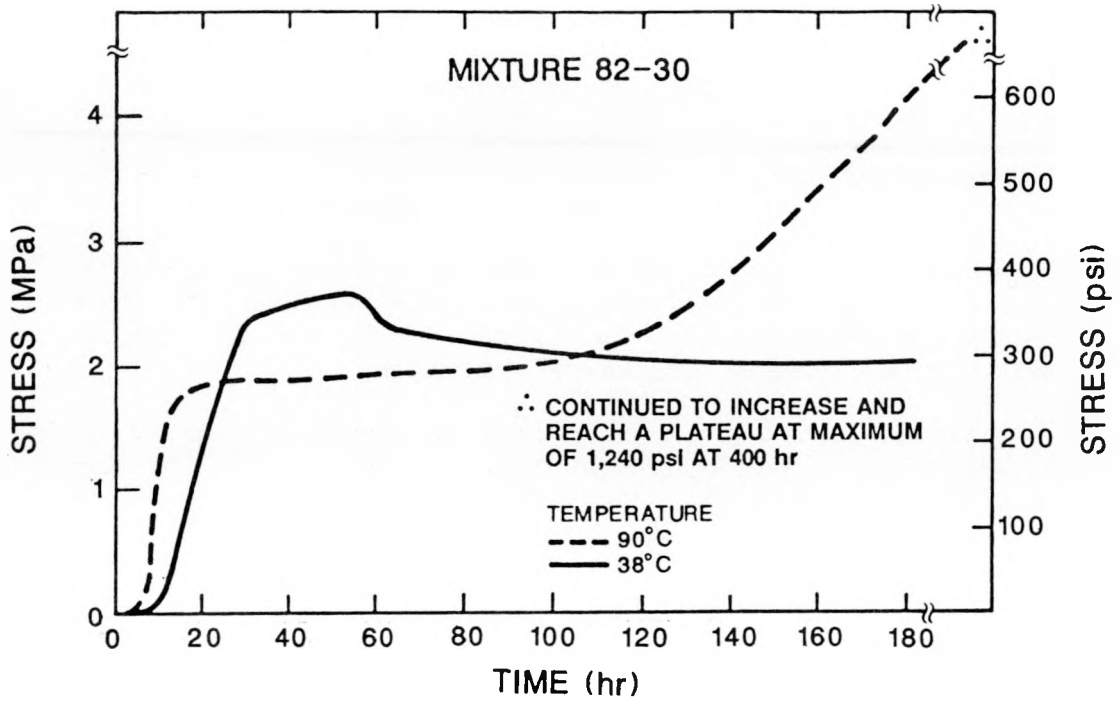

Figure 11. Radial Stresses of Mixture 82-30 (Cured at Different Temperatures and a Pressure of 0.1 MPa)

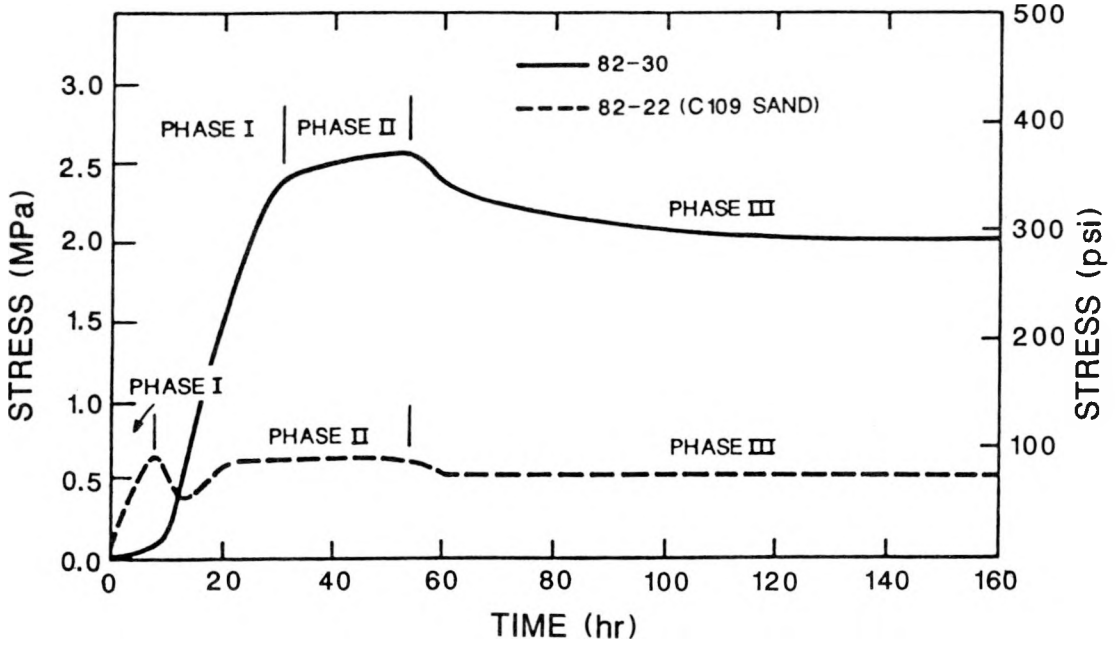

Figure 12. Radial Stresses of Mixtures 82-22 and 82-30 (Cured at 38°C and a Pressure of 0.1 MPa)

simultaneous processes occur during this phase of expansion. The grout starts to harden, fixing to a certain extent its physical integrity and porosity. Several factors affect the behavior of the mortar or grout at this stage of chemical expansion. These include but are not limited to (1) rate of cooling as initial thermal stress is relieved, (2) rate of crystallization of the expansive component(s), (3) setting time and hardening times, and (4) porosity established in the hardened paste.

For mixtures in which initial porosity is low, chemical expansion can become quite large even before the thermal stresses are relieved. This can be seen on the curve for Mixture 82-30 in Figure 12, wherein the initial thermal expansion is totally masked by chemical expansion.

A third phase in the expansion process is characterized by relief of thermal stress. At this stage, controlled by the rates of cooling and of formation of the expansive component(s), the measured stress may drop slightly. This phase appears on Figure 12 at about 60 hr after initiation of the experiments.

In this final phase, the grout has developed appreciable strength and will show only slight expansion or become volumetrically stable (see 3-day strength values for 82-22 and 82-30 in Table 6 and 7-day strength values in Tables 14 and 19). This phase is apparent in Figures 10 and 12, at different curing times depending on the mixture and test conditions.

As a matter of interest, plotting the maximum linear change, from undimensional length-change apparatus, against the radial expansive force (stress measurement) gives the correlation shown in Figure 13. Based on limited data, there appears to be a simple relationship between length change and expansive pressure, regardless of the formulation or curing temperature, provided that the restraint is kept constant.

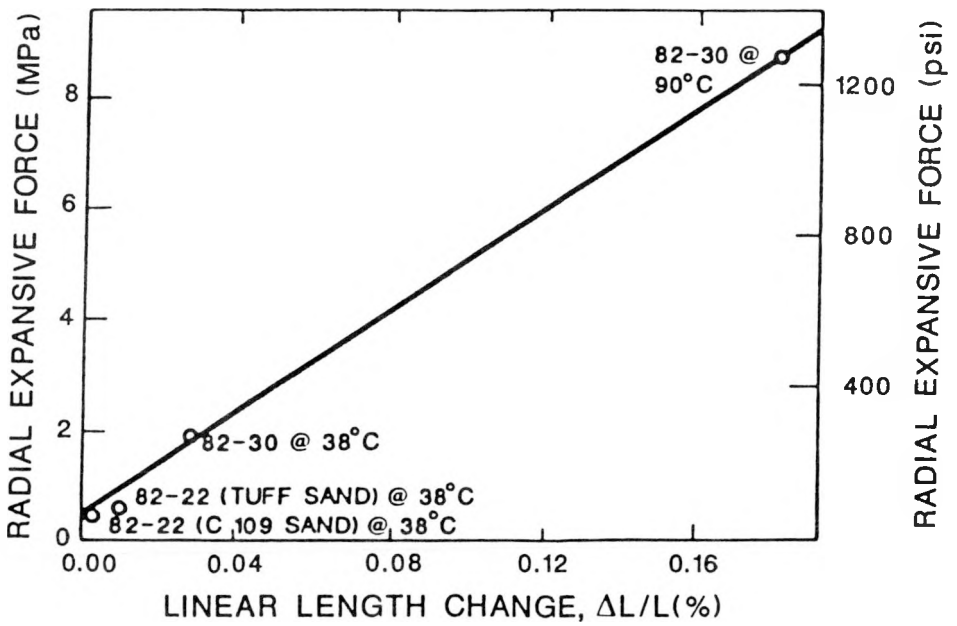

Figure 13. Radial Expansive Force Versus Longitudinal Length Change for Different Mixes

5.5 Interface Properties

For the Phase II bond strength and interface permeability studies, site-specific materials (Topopah Spring tuff, Busted Butte outcrop) were used. These were received as 1 in. (2.54 cm) diameter by 2 in. (5.08 cm) long cores and subsequently cut longitudinally for interface permeability measurements and to 1 in. in length for bond strength tests.

This tuff is devitrified and inhomogeneous in both texture and color. On a macroscopic scale, four different components of the tuff were recognized on the basis of color. The tuff consists of a reddish-brown, finely crystalline groundmass and three distinctive lithic and/or crystalline components, which are the altered equivalents of fragments included in the ash at the time of tuff formation. These four components were separated to determine mineralogic differences among the recognized components. The fraction of lightest color also appeared to be the most porous components of the rock, possibly being only partially welded or nonwelded.

XRD patterns for all four fractions were compared to a pattern for the whole rock, undifferentiated. Although peak intensities differed slightly among fractions, indicating changing proportions of the minerals present, their total mineralogies were identical. The phases identified by XRD include sanidine, cristobalite, quartz, and oligoclase. None of the four fractions contained any zeolite minerals or glassy particles detectable either by XRD or optical petrography. The total chemical composition of this rock (C63) is very similar to other NTS tuff, regardless of mineralogy or rock texture (Appendix A).

The dry bulk density of this welded tuff exceeds 2.2 g/cc, with a porosity of ≤13%. Thermal conductivity is approximately 2.2 W/mK. Permeability to water was measured for cylinders 5 cm long and 2.54 cm in diameter under a confining pressure of 2 MPa and a driving pressure of 1.45 MPa. Measured permeability was 1.7×10^{-7} Darcy, comparable to that of the zeolitic tuff (C48) used in preliminary experiments.

5.5.1 Bond Strength

A number of variables were examined to determine their effects on bond strength. These included pretreatment of the tuff, curing time, curing temperature, and cementitious mixture (either 82-22 mortar or 82-30 grout). To eliminate the uncertainty that could be introduced by using different surface preparations for the tuff surface, the same surface-roughening procedure was used on the Topopah Spring core surfaces (Appendix B-3 contains details).

Other forms of pretreatment of the core surfaces included precoating with either (1) a commercial latex, commonly used to enhance bonding between new grouts or mortars and preexisting surfaces, or (2) a silica sol, Ludox, which was expected to enhance bonding by forming C-S-H rather than $Ca(OH)_2$ at the interface. The two curing temperatures compared were 38 and 90°C, for 7-90 days.

After the pretreatment coating (if any) was applied, core segments for bond-strength samples were placed in 1-in.-diameter brass molds and the

upper half of the mold was filled with the appropriate cementitious mixture. Samples were maintained at >95% relative humidity at the intended curing temperature for 7 days before demolding, to avoid disturbing the interfaces during the first few critical days of curing. After demolding, samples were cured in an unconfined condition for the times and temperatures indicated.

Results of bond-strength measurements for samples cured at 38°C appear in Figure 14. Figure 14 shows that pretreatment with latex or Ludox decreased bonding strength at 38°C curing. Development of strength is more constant at the lower curing temperature, increasing steadily with longer curing time. At 90°C curing (Figure 15), treatment of the tuff surface with either latex or Ludox before casting gives bond strengths that are consistently higher than those with the untreated samples of tuff, when interfaced with Mixture 82-30.

Under all test conditions, bond strength was higher for samples cast with 82-30. At longer curing times, these samples often broke through the grout when tested, rather than separating along the interface. Some of these interfaces were studied via scanning electron microscopy (SEM). This close scrutiny revealed minimal separation of the two components along the interface in the harsh desiccating conditions of the vacuum required for SEM. As observed in Phase I testing, the bond strength increased with an increase in curing time.

5.5.2 Interface Permeability

Samples were tested for permeability at 7, 28, 56, and 90 days of curing. Also, the interface zone was not treated with latex or Ludox. There was no measurable permeability ($<10^{-8}$ Darcy) for any samples at any age or pretreatment, with the single exception of one sample, tested for 7 days, of 82-22 with the tuff (it gave 1.7×10^{-5} Darcy). Considering the results of the permeability data from Phase II discussed here and Phase I (Table 13), a less permeable bond is achieved with the welded tuff and for longer curing times.

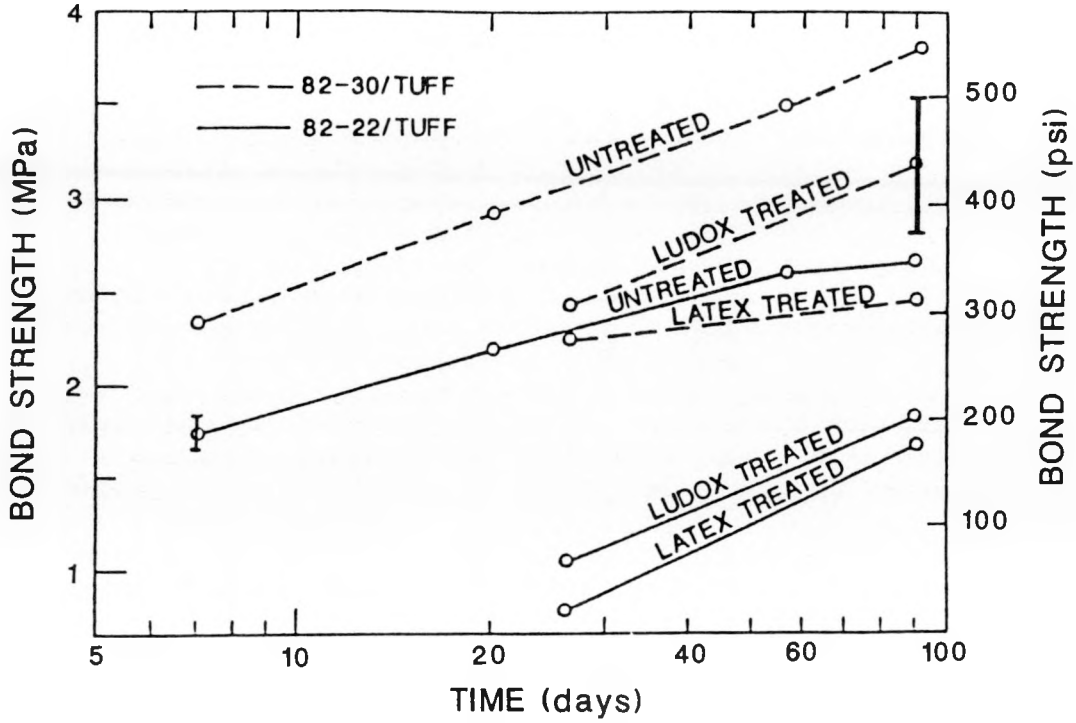

Figure 14. Bond Strength of Mixtures 82-22 and 82-30 (Cured at 38°C and a Pressure of 0.1 MPa, Related to Surface Treatment of C63 Tuff)

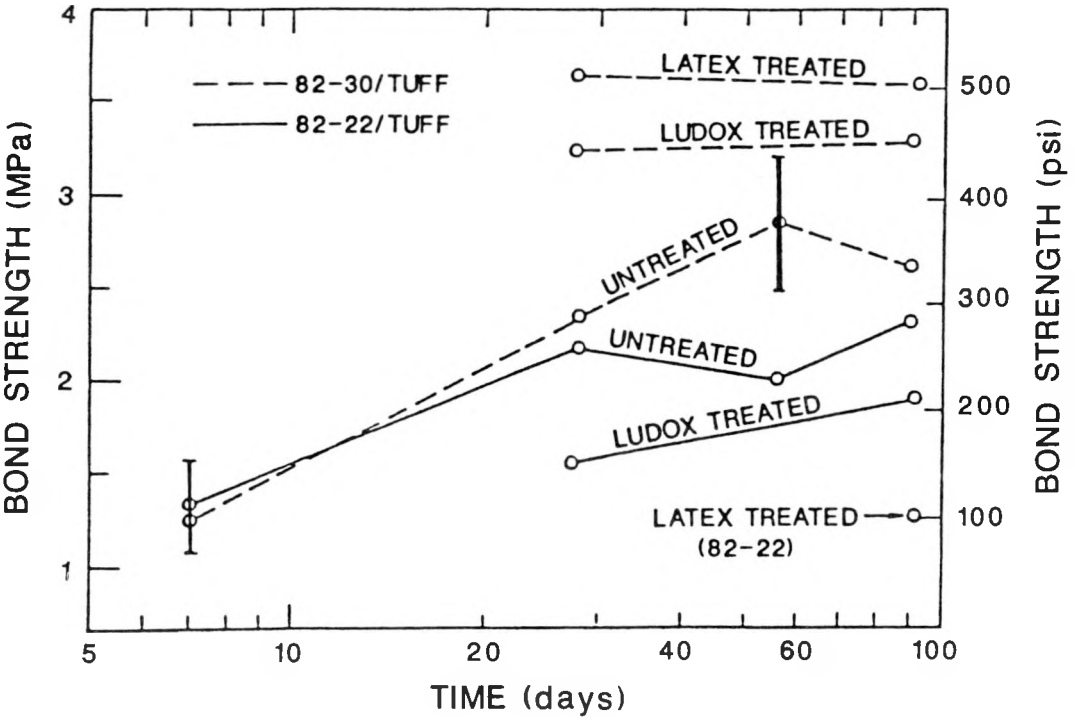

Figure 15. Bond Strength of Mixtures 82-22 and 82-30 (Cured at 90°C and a Pressure of 0.1 MPa, Related to Surface Treatment of C63 Tuff)

6.0 MIXTURE DERIVED FROM EXTENDED-TERM EXPERIMENTS

An additional mixture, a mortar, was designed to retain the most favorable physical and mechanical properties of Mixture 82-22 while modifying its geochemical behavior. The additional criterion factored into the new mortar, 84-12, was to reduce the sulfate content of the leachant. Data are reported here for curing up to 360 days for Mixture 84-12.

6.1 Mixture 84-12

Mix 84-12 is designed to have a reduced sulfate content and high silica with the objective of maintaining an intermediate pH and lessening the potential of the sulfate reacting as a radionuclide complexing agent. As with Mix 82-30 (Table 1), 84-12 is based on a Class H cement. Major modifications in the derivation of 84-12 include a lower percentage of cement, with substitution of slag and increased silica flour; the addition of silica sand to create a sanded grout (82-30 contains no sand); and selection of a Class H cement and no Gypseal to reduce the sulfate composition. As noted in Appendix A (Table A.1), Class H cement has a slightly lower sulfate content than Type K cement. Therefore, the source of the sulfate ion has been reduced; consequently, the amount that can be leached from the mortar is lower. Tests to evaluate the sulfate in the leachant were performed, but no conclusive evidence of sulfate ion reduction was obtained as a result of the short-term (900-hr) duration of the tests (Scheetz and Roy, 1989). However, as mentioned by Scheetz and Roy, reduction in the total amount of sulfate in the mixture would result in a reduction of the total amount of sulfate that could be released but would not necessarily reduce its concentration in the solution while it is being released.

Table 25 lists the components of Mixtures 82-22 and 84-12. Total chemical compositions of 82-22 and 84-12, without regard to sulfate, are plotted in Figure 16. Figure 1 contains comparable data from the eight preliminary mixtures.

6.2 Properties of Mixture 84-12

Mixing of Sample 84-12 followed ASTM C 305 (ASTM, 1985b). Samples were demolded 24 hr after casting and cured at 38°C and immersed in water having a composition similar to J-13 groundwater. Testing of 84-12 continued to 360 days.

Values for compressive strength of cube samples of these mixes are shown in Table 26 for curing times of 7, 14, and 28 days at 38°C. Strength increases rapidly after initial set, exceeding 80 MPa by 7 days. The increase in strength for the Mix 84-12 is about 27% from 7 to 14 days.

Values for static Young's modulus, bulk density, and porosity are also listed in Table 26. Bulk density of 84-12 increases slightly with time and is higher than that of most of the preliminary mixtures, including 82-22. A large percentage of fine-grained components (slag, SiO_2-fume, and SiO_2-flour) and better particle packing would explain the increased density and very low porosity resulting from greater total filling of space. Strength values for both of these mixes at 28 days of curing exceed those of either

Table 25. Components of Mixtures 82-22 and 84-12

Component	Weight Percentage of Mixture	
	82-22	84-12
Type K cement, Z 47	33.8	--
Class H cement, H-10	--	18.6
Mixing water	15.9[a]	15.5[a]
Silica fume	7.3	4.2
Fly ash (low calcium)	8.2	--
Fly ash (high calcium	--	--
Silica flour (5 micron)	--	11.1
Slag	--	23.2
Silica sand	33.8[b]	26.8[c]
Hemihydrate (Gypseal)	--	--
Dispersant--Mighty 150	1.0	0.5
Dispersant--Dowell D65	--	--
Defoamer--Dowell D47	0.005	0.02
w/rs[d]	0.32	0.27

a. Deionized water.
b. ASTM C 109 Ottawa silica sand.
c. Equal parts of (20-40) and (70-140) sands.
d. Ratio of water to reactive solids.

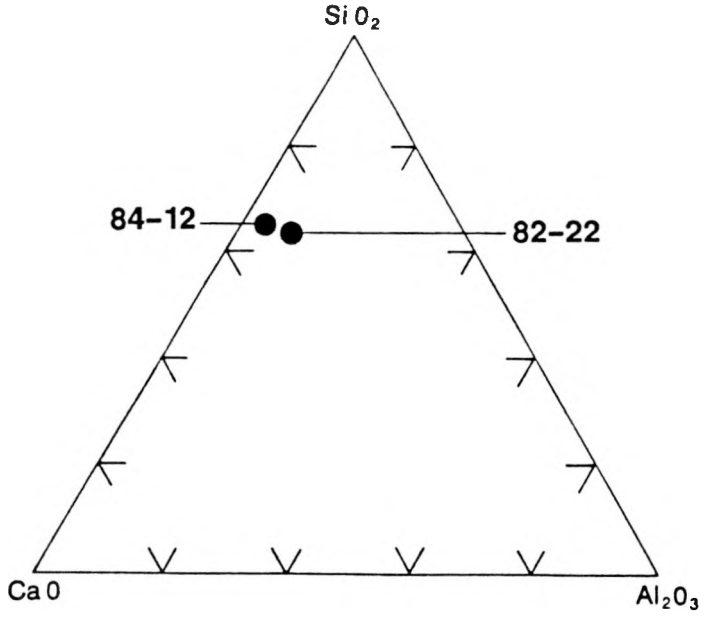

Figure 16. Chemical Compositions of Mixtures 82-22 and 84-12 (SiO_2 = $SiO_2 + P_2O_5$, Al_2O_3 = Fe_2O_3, and CaO = $Na_2O + K_2O + MgO + MnO$)

Table 26. Mechanical/Physical Properties of Mixture 84-12

Curing Time (days)	Compressive Strength (MPa)	Static Young's Modulus (GPa)	Bulk Density (g/cc)	Porosity (%)
7	86.9(3) [6.8]	7.92(3) [0.27]	1.95	8
14	110.0(3) [2.9]	8.27(3) [0.20]	1.98	10
28	117.2(2) [5.5]	8.33(2) [0.46]	2.00	9
56	84.5(1)	8.64(1)	--	--
90	129.7(2) [0.7]	8.62(3) [0.31]	1.97	13
180	141.3(2) [6.9]	9.35(3) [0.71]	2.03	7
360	139.2(3) [5.2]	9.24(3) [0.058]	2.01	9

*Number of samples tested in ( ); one standard deviation, 1σ, given in [ ].

82-22 (96.7 MPa) or 82-30 (98.1 MPa; Table 4), suggesting improvement in strength through these chemical/physical modifications.

Thermal conductivities of samples of the Mix 84-12 are significantly lower than those of 82-22 (Table 27). Its relatively low conductivity probably reflects the higher fly ash content and the higher w/c ratio (Rousan, 1982). Mix 84-12 has been tested to 360 days, with conductivity increasing slightly with time.

6.3 Mineralogy of Sands and Cured Samples of Mix 84-12

XRD of the sands used in Mix 84-12 revealed quartz as the only detectable phase. This was also the case for the sand component of Mix 82-22. Data from size analysis of the sands used in 84-12 are given in Appendix A.

The mineralogy of cured samples was determined by XRD. Quartz and C_3S/C_2S dominate the XRD patterns of Mix 84-12 through 28 days. C-S-H is a major hydrated phase, with minor evidence of calcium hydroxide [$Ca(OH)_2$]. The very low sulfate content of this mixture is reflected in its lack of sulfate-containing hydration products such as ettringite.

Table 27. Thermal Conductivity (W/mK) of Mixtures 82-22 and 84-12

Curing Time (days)	Mixture 82-22	Mixture 84-12
7	2.96	1.42 ± 0.13
14	---	1.53 ± 0.13
28	2.08	1.48 ± 0.09
56	---	1.43 ± 0.12
90	---	1.44 ± 0.16
105	---	---
180	---	1.54 ± 0.09

7.0 SUMMARY AND CONCLUSIONS

The primary use of this study is to provide guidance for future testing in the Yucca Mountain Project repository sealing program. There are two conclusions reached from this study.

- First, the approach used in this study, i.e., developing cementitious materials that have a bulk chemical composition similar to the bulk chemical composition of the tuff environment, is reasonable and should be considered in a future laboratory testing program.

- Second, traditional laboratory tests should be evaluated to determine if reliable material property values can be obtained from the test. Specifically, does the material measurement in the laboratory accurately represent the property of the material as emplaced in the environment, typically a restrained environment.

The first conclusion was reached because desirable properties were achieved by using the approach described in the first conclusion. During the laboratory testing program it was also demonstrated that properties of the materials could be predictably changed through modifications of the mixtures.

In preliminary screening studies (Phase I), several cementitious mortars and grouts were formulated for chemical compatibility with tuffaceous rocks of the NTS. Initial tests of physical and rheological properties of these mixes showed that desirable properties could be achieved. Expansive mixtures showed particular promise, yielding strong, high-density materials with low permeability and adequate bonding to nonwelded tuffs.

Phase II of this work concentrated on two expansive mixtures: a mortar (82-22) high in silica and pumpable grout (82-30) with potential for use in concretes or to meet special sealing requirements. These mixtures were tested for up to 720 days of curing at 38, 60, and 90°C. In general, their physical properties continued to improve throughout the curing period, with some fluctuations in compressive strength values possibly related to curing in an unconfined condition. Permeabilities were consistently very low, commonly less than 10^{-8} Darcy.

Phase II also included long-term experiments of the properties of interfaces between these mixtures and site-specific rocks, which used welded tuff from the Topopah Spring Member of the Paintbrush Tuff. Permeabilities of these interface samples were less than or equal to those measured for the tuff alone (on the order of 10^{-7} Darcy or less). A general increase of bond strength with curing time was observed for both formulations. Mixture 82-30 gave higher bond, tensile strengths, achieving over 3.45 MPa at 90 days of curing at 38°C. Pretreatment of the tuff surface before casting the cement gave higher bond strengths at 90°C curing, possibly as a result of an accelerated reaction at the interface with this sand-free formulation. However, this pretreatment decreased bond strength for samples cured at 38°C.

Another mixture, 84-12, incorporates a geochemical requirement together with maintaining the physical and mechanical properties of Mix 82-22. The geochemical requirement was reduction of the total amount of sulfate that could be released. This requirement was achieved by reducing the amount of sulfate added to the original mixture. Reducing the amount of Portland cement and using silica flour, silica fume, fly ash, and slag additives to maintain a high content of reactive silica (and alumina) with <20% (by weight) of cement in the total formulation achieved this requirement. Preliminary data for Mixture 84-12 suggest attainment of a dense, pumpable product that hydrates to a solid of very high strength and low porosity, with a chemical composition that should make it highly compatible with NTS tuffs.

The bases for the second conclusion were a number of observations made during the testing program. These observations are given below and should be considered in planning future laboratory testing.

- Removal of samples from their molds after 24 hr may be inappropriate for cementitious materials that continue to expand. Expansion in an unrestrained environment can affect the properties measured in the laboratory. Results from this study indicated that unconfined compressive strengths fluctuated at different times and under various testing conditions. This fluctuation was attributed in part to the development of ettringite which expanded for the unconfined samples. Other properties were also affected. For example, when the unconfined compressive strength was lower than expected, corresponding changes occurred in the thermal conductivity, porosity, and density values. The thermal conductivity and density values were low when the unconfined compressive strengths were low; whereas, the porosity values were higher. If any of these values are determined to be significant from a performance viewpoint, then modeling and testing in the laboratory should parallel the conditions encountered in the field, as much as possible recognizing that emplacement of seal materials in the actual emplacement environment could also cause variations in the properties of the seal materials.

- Variations in the temperature and pressure conditions in the laboratory will affect the apparent expansion or contraction of the cementitious sample as it cures following initial mixing. Because the residual expansion may affect the overall performance of the seal under some applications where a good interface bond is necessary, selection of the correct environmental conditions would be required in the laboratory.

- Textural differences between rocks can potentially affect the interface permeability of a composite sample of the rock with the cementitious materials. Therefore, future testing should monitor the texture of the rock.

- The intention of this study was to perform several of the more common types of analyses to gain an understanding of the properties of the grouts and mortars. For each type of analysis, only a limited number of replicate samples were run. In some cases, only one sample was used to determine a specific property. It became apparent in the case of the

unconfined compressive strength that three samples were inadequate to obtain reliable material properties. Therefore, as with any laboratory testing program, a statistically significant number of samples must be run to account for experimental error and variations in preparation and testing of samples.

- The curing/storage conditions in the laboratory should be carefully monitored to represent the environment of the emplaced material. During one portion of this study, it was observed that samples used to determine the dynamic modulus were cured at high humidity and not immersed in a curing solution. At one point during the storage of the sample it was noticed that water under the storage pan had evaporated and the sample had dried, potentially causing microcracking of the sample. This storage condition significantly reduced the dynamic modulus of the sample.

- Although not conclusive, permeability measurements on the cementitious materials were not noticeably affected by the temperature or other storage conditions.

- Under certain conditions bond strength between the rock and the cementitious materials may be enhanced by treatment of the rock surface.

8.0 REFERENCES

ASTM (American Society for Testing and Materials), 1985,

a. "Standard Test Method for Compressive Strength of Hydraulic Cement Mortars (Using 2-in. or 50-mm Cube Specimens)," ASTM C 109-84; (NNA.900316.0014)

b. "Standard Method for Mechanical Mixing of Hydraulic Cement Pastes and Mortars of Plastic Consistency," ASTM C 305-82; (NNA.890713.0192)

c. "Standard Specification for Standard Sand," ASTM C 778-80a; (NNA.890522.0225)

in Volume 04.01 Cement; Lime; Gypsum, Philadelphia, PA.

ASTM (American Society for Testing and Materials), 1985,

d. "Standard Test Method for Fundamental Transverse, Longitudinal, and Torsional Frequencies of Concrete Specimens," ASTM C 215-85; (NNA.890713.0190)

e. "Standard Test Method for Specific Gravity, Absorption, and Voids in Hardened Concrete," ASTM C 642-82; (NNA.890713.0191)

in Volume 04.02 Concrete and Mineral Aggregates, Philadelphia, PA.

Barnes, P. (ed.), 1983, Structure and Performance of Cements, Applied Science Publishers, Essex, England. (NNA.890522.0209)

DOE (U.S. Department of Energy), 1988, Site Characterization Plan, Consultation Draft, Yucca Mountain Site, Nevada Research and Development Area, Nevada, Office of Civilian Radioactive Waste Management, Washington, DC. (HQS.881201.0002)

Fernandez, J. A., 1985, Repository Sealing Plan for the Nevada Nuclear Waste Site Investigations Project, Fiscal Years 1984 through 1990, SAND84-0910, Sandia National Laboratories, Albuquerque, NM. (NNA.870407.0030)

Grutzeck, M. W., D. M. Roy, and B. E. Scheetz, 1981, "Microstructures of High-Lime Fly Ash Cementitious Mixes," Cem. Concr. Res., Vol. 11, No. 2, pp. 291-294. (NNA.900316.0015)

GSA (The Geological Society of America), 1966, Handbook of Physical Constants, S. P. Clark, Jr., ed., Memoir 97, New York, NY. (NNA.890327.0070)

Johnstone, J. K., R. R. Peters, and P. F. Gnirk, 1984, Unit Evaluation at Yucca Mountain, Nevada Test Site: Summary Report and Recommendations, SAND83-0372, Sandia National Laboratories, Albuquerque, NM. (NNA.870519.0052)

Lea, F. M., 1971, The Chemistry of Cement and Concrete, Chemical Publishing Co., Inc., New York, NY. (NNA.890713.0195)

Nakagawa, Z., E. L. White, and D. M. Roy, 1982, "Rheological and Physical Properties of Magnesium Oxide and Silica Fume-Modified Cement Mortars Cured at High Temperature," Scientific Basis for Nuclear Waste Management VI, Materials Research Society Symposia Proceedings, Elsevier Science Publishing Co., Inc., New York, NY, Vol. 15, pp. 97-104. (NNA.890522.0251)

Rousan, A. A., 1982, A Methodology for Thermal Characterization of Cementitious Materials, Ph.D. Thesis, Pennsylvania State University, University Park, PA. (NNA.890327.0078)

Roy, D. M., 1980, "Geochemical Factors in Borehole and Shaft Plugging Materials Stability," in Proceedings of the Workshop on Borehole and Shaft Plugging, Organization for Economic Co-operation and Development Nuclear Energy Agency and U.S. Department of Energy, Columbus, OH, 7-9 May 1980, pp. 368-384. (NNA.890522.0255)

Roy, D. M., M. W. Grutzeck, and P. H. Licastro, 1979, Evaluation of Cement Borehole Plug Longevity, ONWI-30, Office of Nuclear Waste Isolation, Battelle Memorial Institute, Columbus, OH. (NNA.890327.0079)

Sarkar, A. K., M. W. Barnes, and D. M. Roy, 1980, Longevity of Borehole and Shaft Sealing Materials. I: Thermodynamic Properties of Cements and Related Phases, A Topical Report for Office of Nuclear Waste Isolation, ONWI-201, Materials Research Laboratory, The Pennsylvania State University, University Park, PA. (NNA.900316.0016)

Scheetz, B. E., and D. M. Roy, 1989, Preliminary Survey of the Stability of Silica-Rich Cementitious Mortars [82-22 and 84-12] with Tuff, Los Alamos National Laboratory, Los Alamos, NM. (NNA.870827.0004)

Soroka, I., 1979, Portland Cement Paste and Concrete, Chemical Publishing Co., Inc., New York, NY. (NNA.890522.0219)

Stanton, T. E., 1944, Tests Comparing the Modulus of Elasticity of Portland Cement Concrete as Determined by the Dynamic (Sonic) and Compression (secant at 1000 psi) Methods, ASTM Bulletin 131, American Society of Testing and Materials, Philadelphia, PA. (NNA.890522.0220)

Wakeley, L. D., and D. M. Roy, 1982, "A Method for Testing the Permeability Between Grout and Rock," Cem. Concr. Res., Vol. 12, No. 4, pp. 533-534. (NNA.890327.0040)

White, E. L., and D. M. Roy, 1982, "Rheological Properties of Cement Slurries, Mortars, and Grouts," Symposium M. Rheology of Fresh Concrete: Basic Surface and Colloid Physics, Special Issue, Materials Research Society, University Park, PA, pp. 108-117. (NNA.900316.0017)

Winograd, I. J., and W. Thordarson, 1975, Hydrogeologic and Hydro-chemical Framework, South-Central Great Basin, Nevada-California, With Special Reference to the Nevada Test Site, U.S. Geological Survey, USGS-PP-712-C, U.S. Dept. of Interior, Washington, DC. (NNA.870406.0201)

Zimmerman, R. M., and W. C. Vollendorf, 1982, Geotechnical Field Measurements, G-Tunnel, Nevada Test Site, SAND81-1971, Sandia National Laboratories, Albuquerque, NM. (HQS.880517.1720)

APPENDIX A

ANALYSES OF MIXTURE COMPONENTS AND MATERIALS

Table A.1. Chemical Analyses of Cements and Reactive Compounds Used in Eight Preliminary Mixtures

	Cement				Silica Fume					Fly Ash		
	Type K	Class H								Low Ca	High Ca	Slag
Component	Z47 (%)	H-07 (%)	H-08 (%)	H-10 (%)	B27 (%)	B31 (%)	B58 (%)	B59 (%)	B60 (%)	B25 (%)	B62 (%)	B19 (%)
SiO_2	20.1	22.3	22.27	22.24	96.0	94.3	95.21	94.54	99.23	50.2	36.8	32.68
Al_2O_3	4.11	3.84	3.60	3.58	0.10	0.36	0.04	0.10	0.261	27.0	18.1	8.34
TiO_2	0.22	0.19	0.17	0.18	<0.1	<0.1	0.01	<0.05	0.034	1.40	1.55	0.42
Fe_2O_3	3.19	3.80	4.01	3.94	<0.1	0.66	0.04	0.20	0.071	13.8	6.21	1.18
MgO	4.18	2.08	2.87	3.87	0.13	1.42	0.28	0.26	<0.01	0.84	4.74	8.85
CaO	62.26	64.78	64.40	62.99	0.12	0.27	0.10	<0.05	0.022	1.82	27.83	44.64
MnO	0.048	0.015	0.02	0.022	0.010	0.023	0.010	0.007	*	0.034	0.039	0.25
Na_2O	0.14	0.09	0.15	0.13	0.1	0.76	0.12	0.05	*	0.24	1.22	0.25
K_2O	0.45	0.49	0.57	0.53	0.45	1.112	0.43	0.45	*	2.45	0.41	0.34
P_2O_5	0.12	0.14	0.11	0.08	0.07	0.05	0.05	0.09	*	0.49	0.94	0.03
SO_3	4.59	1.92	1.99	1.92	*	*	0.41	0.44	*	*	1.90	3.08
LOI	2.04	0.43	*	0.66	*	*	3.36	3.57	0.381	*	0.55	*
CO_2	*	0.21	0.48	*	*	*	*	*	*	*	*	0.57
BaO	0.05	0.03	*	0.02	*	*	*	<0.05	*	0.14	0.60	*
SrO	0.05	0.07	0.06	0.06	*	*	*	<0.05	*	0.11	0.30	0.06
Totals	101.55	100.39	100.70	100.22	96.98	98.96	100.06	99.71	100.00	98.52	101.19	100.69

*No analyses performed.

Table A.2. Predominant Components of Mixing/Curing Water[a] in mg/l

Component	E-22[b]	E-25[c]	J-13[d]
SiO_2	41.0	31.6 [32]	31.0 [30] [57]
Ca^{2+}	28.0	3.51 [13]	14.0 [11.5] [12]
Mg^{2+}	10.4	<1.0 [1.0]	2.1 [1.76] [2.1]
Na^{+}	89.0	100.0 [99]	51 [45] [42]
K^{+}	7.3	7.5 [6.4]	4.9 [5.3] [5.0]
HCO_3^{-}	e	e [199]	120.0 [ND] [124]
SO_4^{2-}	e	130.0 [34]	2.2 [18.1] [17]
Cl^{-}	e	35 [32]	7.5 [6.4] [7.1]
pH	9.8	7.3 [7.3]	7.1 [6.9] [7.2]

a. Waters E-22, E-25, and J-13 were formulated in the laboratory.
b. Estimate of chemical composition.
c. Based on chemical composition of water taken from Well 73-66 and depth interval of 77-693 ft (Winograd and Thordarson, 1975, p. C107). Values in [ ] represent values taken from Thordarson's report.
d. Based on chemical composition of water taken from Well J-13. The numbers in first set of brackets represent values taken from Ogard and Kerrisk (1984, pp. 9-10). The numbers in the second set of brackets represent values taken from Benson and McKinley (1985, p. 5).
e. No analysis performed.

Table A.3. Chemical Analyses of Tuff Samples From G-Tunnel and Yucca Mountain

Sample No.[a]	Nonzeolitic C63,65[b] (%)	Zeolitic C48x[c] (%)	Zeolitic C48[c] (%)
SiO_2	73.2	70.8	75.04
Al_2O_3	12.1	9.55	10.0
TiO_2	0.10	0.34	0.28
Fe_2O_3	1.10	2.75	2.71
MgO	0.25	0.67	0.20
CaO	2.10	1.87	0.32
MnO	0.112	0.114	0.105
SrO	---	0.01	<0.05
BaO	---	0.01	<0.05
Na_2O	3.65	1.02	2.13
K_2O	4.89	3.33	6.74
P_2O_5	0.11	0.01	0.09
SO_3	<0.01	0.06	0.03
LOI (950°C)	2.24	9.03	1.67
Totals	99.85	99.56	99.32

a. PSU/MRL code numbers and analyses.
b. Topopah Spring Member (Busted Butte Outcrop).
c. G-Tunnel tuff.

Table A.4. Size Analyses of Coarse Sand Components Used in Mixture 84-12

Sieve Size	PSU #C90 Sand* (20-40)
#16	100% passes through
#20	99% passes through
#40	95% retained
#50	1% passes through

*Acquired from commercial source; used in Mix 84-12.

REFERENCES

Benson, L. V., and P. W. McKinley, 1985, Chemical Composition of Groundwater in the Yucca Mountain Area, Nevada, 1971-84, USGS-OFR-85-484, U.S. Geological Survey, Denver, CO. (NNA.890522.0210)

Ogard, A. E., and J. F. Kerrisk, 1984, Groundwater Chemistry Along Flow Paths Between a Proposed Repository Site and the Accessible Environment, LA-10188-MS, Los Alamos National Laboratory, Los Alamos, NM. (NNA.870406.0021)

Winograd, I. J., and W. Thordarson, 1975, Hydrogeologic and Hydrochemical Framework, South-Central Great Basin, Nevada-California, with Special Reference to the Nevada Test Site, USGS-PP-712C, U.S. Dept. of Interior, Washington, DC. (NNA.870406.0201)

APPENDIX B

TEST PROCEDURES AND REFERENCE STANDARDS

CONTENTS

FIGURES

TABLES

B-1. LONGITUDINAL LENGTH CHANGE

B-1.1 Apparatus

The equipment used for longitudinal length-change determination is shown diagrametrically in Figure B-1. It consists of a 1 x 1 x 7.25-in. sample cell that offers restraint in the radial direction. The cell assemblage is maintained within a pressure vessel capable of atmospheric pressure to 3,000 psi. An outer furnace assembly permits controlled temperatures from ambient to 100°C.

Length change is determined by use of a linear variable displacement transducer (LVDT) and its accessory signal conditioner/amplifier. This transducer has an accuracy of ±0.0002 in.

B-1.2 Calibration

An initial cell constant was determined for the system to compensate for heat/dimensional changes of the mold and pressure vessel. This was accomplished by using a 303 stainless steel bar of known thermal properties. Derivation of a typical cell factor is shown in Table B-1.

In addition to establishing the cell factor, the LVDT voltage output versus displacement is determined before each experiment. This is accomplished by moving the LVDT sensing head assembly vertically with a precision micrometer screw and recording the resultant output voltage. A typical calibration curve is presented in Figure B-2.

B-1.3 Test Procedure

The grout is prepared according to ASTM procedure and carefully placed in the mold. The mold is then placed in the high-pressure curing cell, which has been set for the predetermined experimental curing conditions (temperature and relative humidity). The cell is pressurized at this point in time if other than atmospheric tests are being conducted. The mechanism measuring the expansion or contraction of the sample is placed on top of the exposed sample. Because of the weight of this mechanism some time is required for the movement of this mechanism to stabilize and reflect the "actual" contraction or expansion of this tested sample. In Figures B-2 and B-3, approximately one hour is required to reach stabilization.

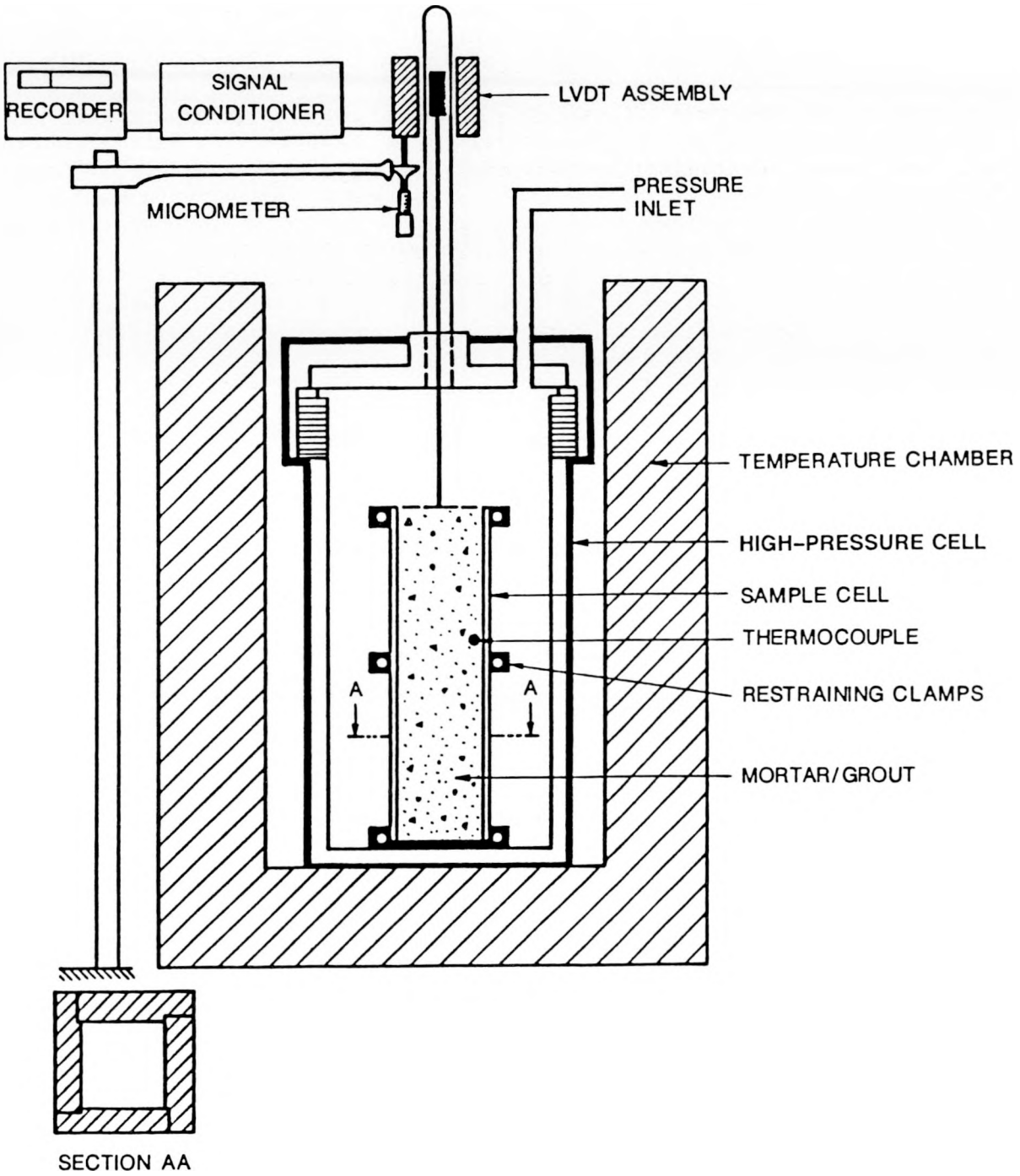

Figure B-1. Apparatus for Longitudinal Length-Change Determination

Table B-1. Physical Constants and Test Results of the Steel Bar for Calibrating the Longitudinal Length-Change Equipment

Calibration Standard: Stainless steel type 303
Mean coefficient of thermal expansion: 10.4 in./in./°F x 10^{-6} [32-1200°F] 18.7 cm/cm/°C x 10^{-6} [0-649°C]
Specific heat: 0.12 BTU/lb/°F [32-212°F] 0.12 KCal/kg/°C [0-100°C]
Length at 24°C (room temperature): 7.821 in.
Temperature limits of the experiments: 38-67°C
Initial length at starting temperature: 7.832 in.
Length change between experimental temperature limits:
(calculated) 0.0042398 in.; (measured) 0.0071823 in.
Length change resulting from cell: 0.0029425 in.
Cell factor: 1 x 10^{-4} in./°C

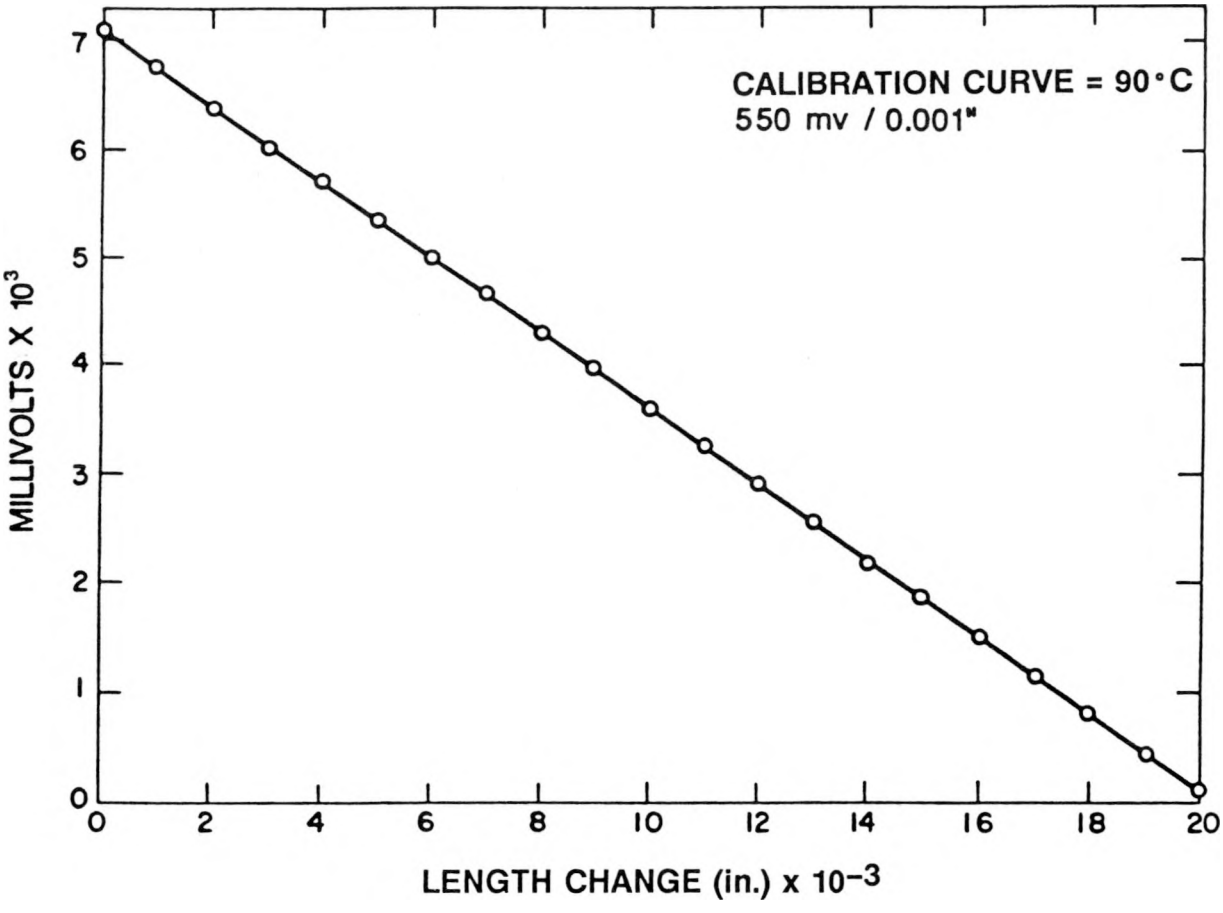

Figure B-2. Example Calibration Curve for LVDT Voltage Output versus Displacement

B-2. EXPANSIVE PRESSURE

B-2.1 Apparatus

The apparatus used for expansive force determination consists of a steel cylinder held by base and top plates, as shown in Figure B-3. Both bottom and top plates are provided with O rings to ensure effective sealing of the steel cylinder during calibration. This design of the cell eliminates the hydrostatic load in the vertical direction on the steel cylinder, i.e., any internal pressure on top and bottom pieces is compensated by the holding forces of the external bolts. The physical and mechanical characteristics of the steel cylinder are shown in Table B-2.

Table B-2. Physical and Mechanical Characteristics of the Steel Cylinder Used in Stress Measurement

Modulus of elasticity, 10^6 psi
tension: 26.0
compression: 26.0
torsion: 9.5
Poisson's ratio: 0.32
Coefficient of linear expansion (in./in./°F x 10^{-6}) at 70-200°F: 7.7
Thermal conductivity (BTU/in./hr/sq ft/°F), at 70°F: 151.0; at 200°F: 167.0
Specific heat (BTU/lb/°F), at 70°F: 0.102; at 200°F: 0.105
Physical dimensions
length: 9.0 in.
internal diameter: 1.60 in.
external diameter: 1.84 in.

A 90° rossette strain gage is attached to the central part of the outer surface of the cylinder. The gage is connected to a signal conditioner and recorder. Both radial and longitudinal strains are recorded continuously. The physical characteristics of the strain gage are shown in Table B-3.

An alumel-chromel thermocouple is attached to the outer surface of the cylinder, in close proximity to the strain gage, to record any temperature variations and establish the necessary corrective factors for the temperature-induced strains. The entire cell is contained in a chamber, adjusted to the desired experimental temperature. The chamber is surrounded by a heated water jacket to ensure constant temperature and to avoid the effect of radiant pulses of the heating elements on the strain gage output. The temperature control accuracy is ±0.5°C for the entire chamber.

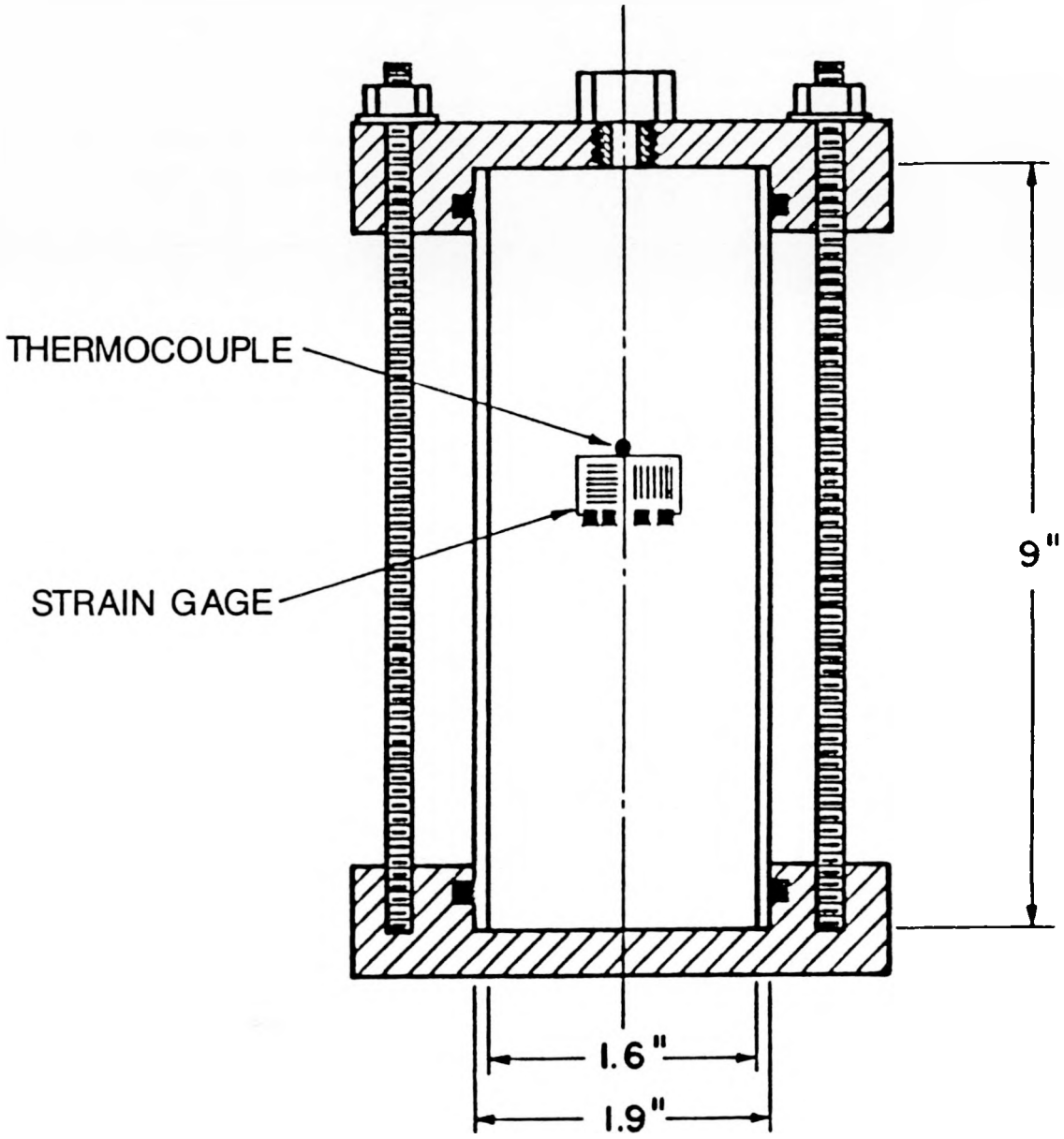

Figure B-3. Apparatus for Determination of Expansive Force

Table B-3. Physical Characteristics of the 90° Rossette Strain Gage

Type:	CEA-06-125UT-120
	Micro-measurements Group, Raleigh, NC
	Resistance (ohm): 120.00 ± 0.4%
	Gage factor (75°F): 2.025 ± 0.5%
Transverse sensitivity (K_t %)*:	Radial +1.4%; Longitudinal +0.6%

*The values of transverse sensitivities gave very minute correction factors to the recorded strains, which are considered the true values of strains in both directions.

B-2.2 Significance of the Design of the Stress-Measurement Experiments

It is assumed that the compliance of the model in the laboratory (the relationship of hoop strain to interface stress) is the same as that for the prototype. The compliance is given by

$$\varepsilon_\theta/P_i = \mu_i/(r_i P_i) = 1/2G_R \quad , \qquad [B\text{-}2.1]$$

where

ε_θ = hoop strain
P_i = interface stress
μ_i = radial displacement
r_i = radius
G_R = modulus of rigidity of the rock.

For a thick-walled cylinder under plane strain conditions, the compliance was developed as

$$\varepsilon_\theta/P_i = \mu_i/(r_i P_i) = R_S/E_S$$

$$R_S = 1 + r_1^2/r_0^2/1 - r_1^2/r_0^2 + \nu_s^2 - 2\nu_s^2/r_0^2/r_1 - 1 \qquad [B\text{-}2.2]$$

where

E_S = Young's modulus of the cylinder
r_1 = inner radius of the cylinder
r_0 = outer radius of the cylinder
ν_s = Poisson's ratio of the cylinder.

Equating the compliance values [1] (for rock) and [2] (for cylinder) results in

$$R_S/E_S = 1/2G_R \quad .$$

Solving for r_0/r_i,

$$r_0/r_i = \left| \frac{1/2G_R + 1 - \nu_s/E_S}{1/2G_R - 1/2G_S} \right|^{1/2} \quad , \qquad \text{[B-2.3]}$$

where

G_S = modulus of rigidity of the cylinder.

The ratio of outside to inside radius is shown in Figure B-4.

Applying the relationship $G = E/2(1 + \nu)$, where G is the modulus of rigidity (shear modulus), E is the Young's modulus (elastic modulus), and ν is the Poisson's ratio (0.22-0.30), we find that G = 16.5 GPa. From Equation B-2.3 or Figure B-4, it can be seen that r_0/r_i = 1.18, i.e., the ratios of outer radius to inner radius for the steel cylinder to be used to simulate the candidate host rock (tuff) is 1.18. For that reason the steel cylinder was chosen of internal radius 0.8 and in outer radius 0.95 in., so that 0.95/0.8 = 1.19. The steel cylinder was confined to hinder any vertical change in the dimensions of that cylinder resulting from frictional forces, a condition that simulates a tuff borehole. On the other hand, the length of the cylinder was chosen (length/internal diameter ratio = 5.6) so that the recorded strains in the middle of the cylinder will not be affected by the end conditions.

B-2.3 Experimental Procedure

B-2.3.1 Calibration

Before each experiment, the steel cylinder-strain gage combination is exclusively calibrated. These procedures allow giving precise measurement of the actual stresses exerted by the grout inside the steel cylinder and save time in calculating the correct strains. They also allow applying corrective terms for different conditions to the recorded strains to obtain the true stresses applied by the grout on the cylinder.

1. Checking the accuracy of the equipment

   The electronics of the system are checked for calibration and necessary adjustments are made, when needed, so that accurate readings are obtained.

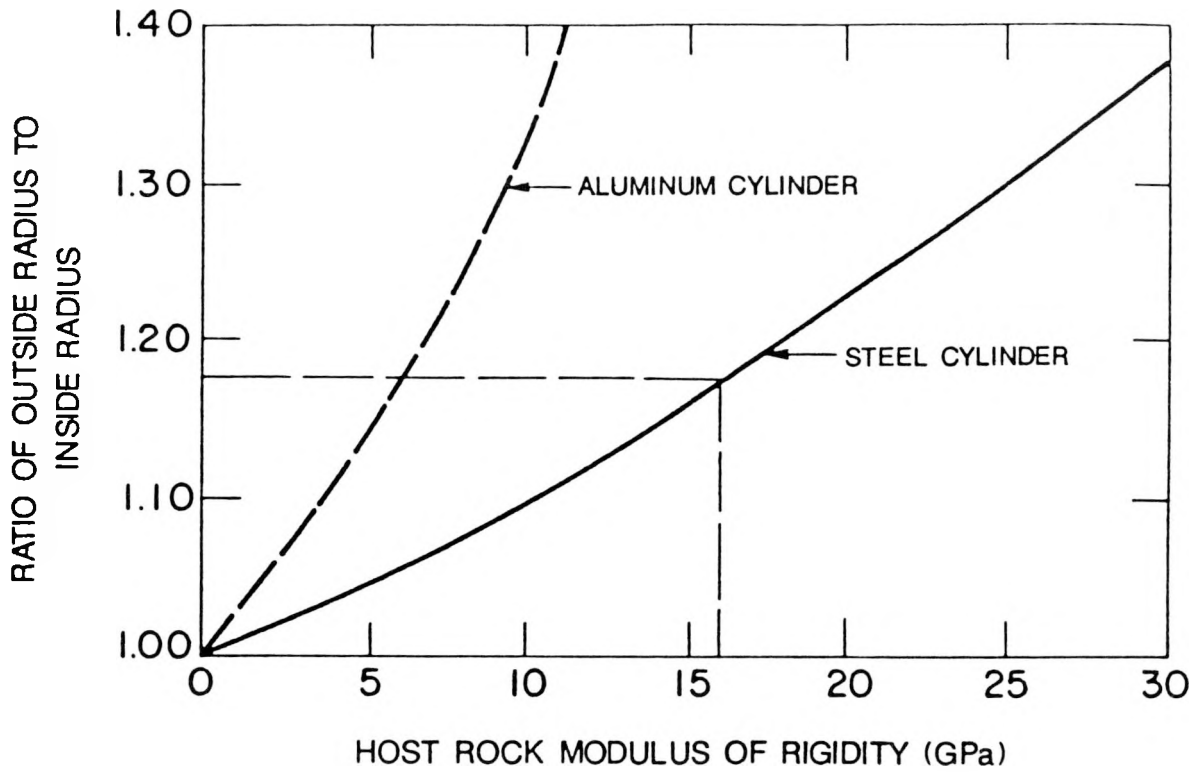

Figure B-4. Ratio of Outer to Inner Radii of Cylinders Related to Modulus of Rigidity of Host Rock

2. Stress calibration

The steel cylinder is filled with water, the upper cap is placed, and the four outer bolts are tightened to a torque of 10 lb-in. each. The upper cap is connected to a water pump that enables pressurizing water inside the cylinder. The flow rate of the water pump is adjusted to 0.60 ml/min.

The entire assembly is placed inside the curing chamber that is adjusted to the temperature at which the stress measurement is to be made. The assembly is left, with the strains and temperature of the surface of the steel cylinder being recorded, until both strain and temperature show a constant reading. Calibration is achieved by pressurizing water at successively increasing pressure increments and recording the corresponding outputs of the strain gage. Calibration curves were constructed and examples are shown in Figures B-5 and B-6. The radial strain is recorded as positive output indicating tension, whereas the longitudinal strain is negative, indicating compression. The ratio of longitudinal strain to radial strain is equal to 0.327, which equals the Poisson's ratio of the steel material of the cylinder.

The hydrostatic internal pressure exerted by the fluid on the top and bottom plates (which might affect the radial strain) is totally compensated by the holding forces of the outer bolts. Thus, the radial strain calibration corresponds to the internal radial pressure without being affected by vertical forces. Therefore, the recorded strains, when the grout is placed inside the cylinder, could be directly converted to radial pressures using the calibration values and those will represent the true radial pressures exerted by the grout.

The results of stress calibration of different cylinder/gage combinations are shown in Table B-4.

3. Temperature calibration

The steel cylinder is filled with water and a heating element is inserted. Heat is applied in successive increments with constant slow rate of heating. The recorded strains are taken after a sufficiently long period of time to ensure equilibrium attainment. The resultant temperature coefficient of induced strains is calculated and the values for different cylinders are included in Table B-4. However, the temperature coefficients shown in Table B-4 cover only a limited range of temperature variations where the temperature-induced strain varies linearly with temperature. For a wider range of temperature variations, the values deviate from linearity and in such cases precise calibration curves should be constructed. An example of such a calibration curve is shown in Figure B-7 for one steel cylinder/strain gage combination.

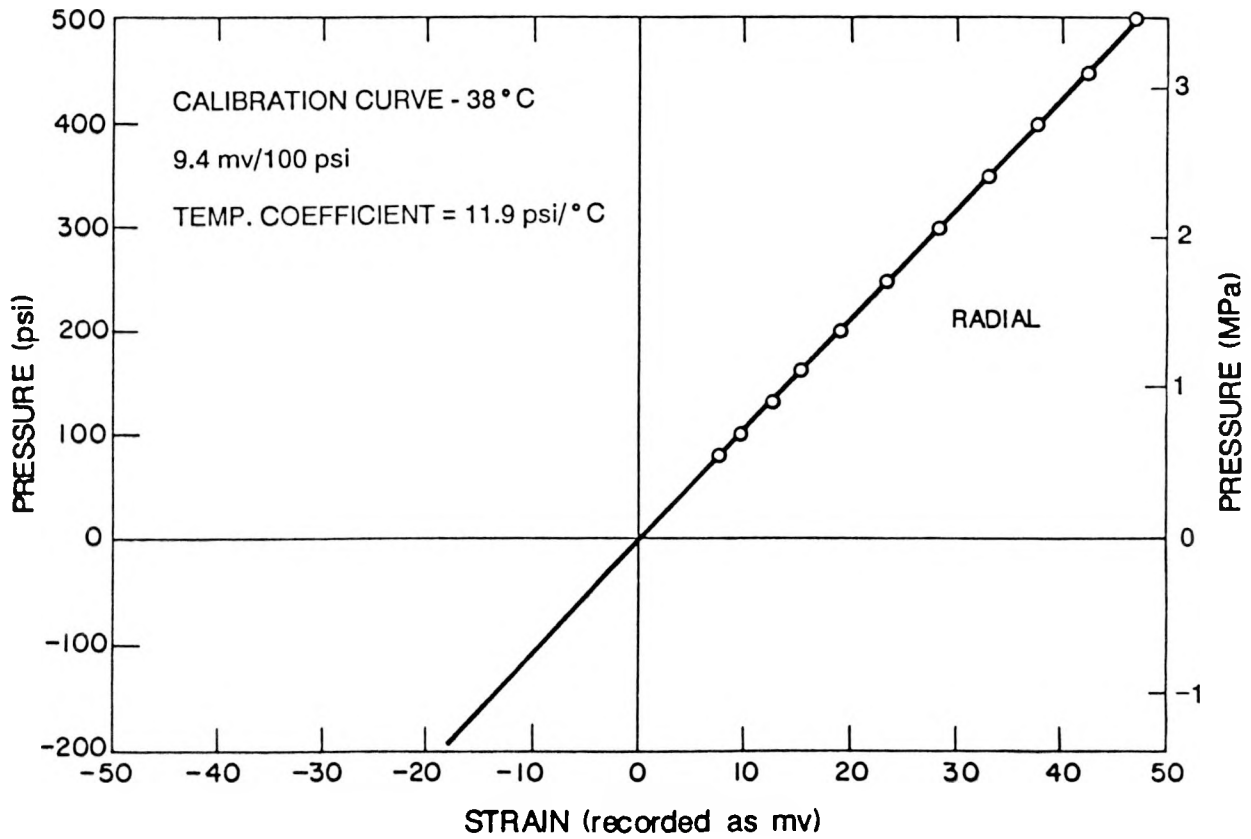

Figure B-5. Example Calibration Curve for Radial Expansion

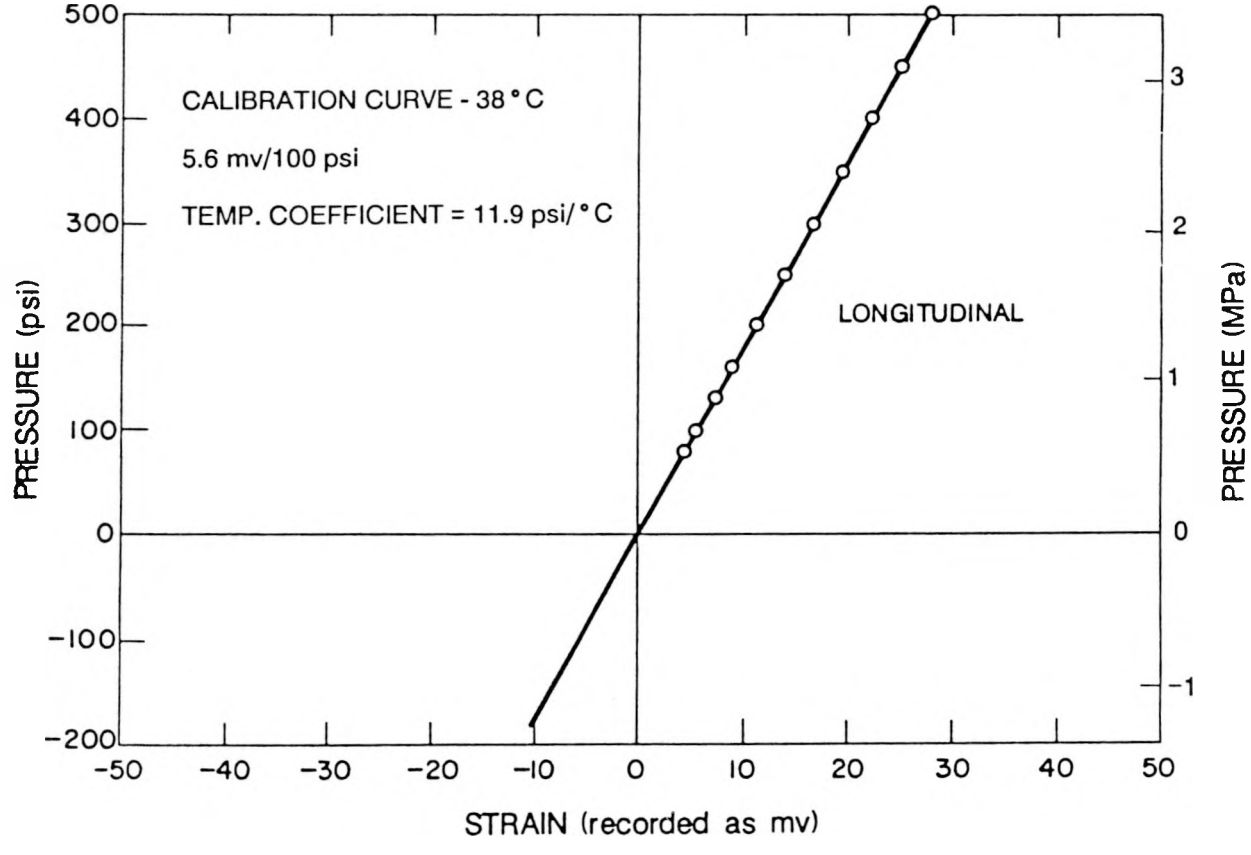

Figure B-6. Example Calibration Curve for Longitudinal Expansion

Table B-4. Results of Calibration for Steel Cylinder/Strain Gage Combinations

	Strain (mvolts/psi x 10^{-2})	Coefficient of Temperature-Induced Strains
Cylinder I (38°C)		
Radial	8.88	11.50
Longitudinal	-5.32	14.34
Cylinder II (38°C)		
Radial	9.40	11.90
Longitudinal	-5.60	11.90
Cylinder III (90°C)		
Radial	8.88	11.50
Longitudinal	-4.96	11.50

These temperature coefficients and/or temperature calibration curves are used to correct the recorded strains, to obtain stress curves normalized for experimental temperature. Examples of such corrections are shown in Figure B-8. All results presented in the present investigation are corrected for temperature variations.

After calibrating the steel cylinder/strain gage combination for stresses and temperature, the total assembly remains unloaded for a period of time to ensure stability of the system with no drift in the strain readings. The cell is then loaded with cement grout and placed in the curing chamber adjusted to the desired temperature.

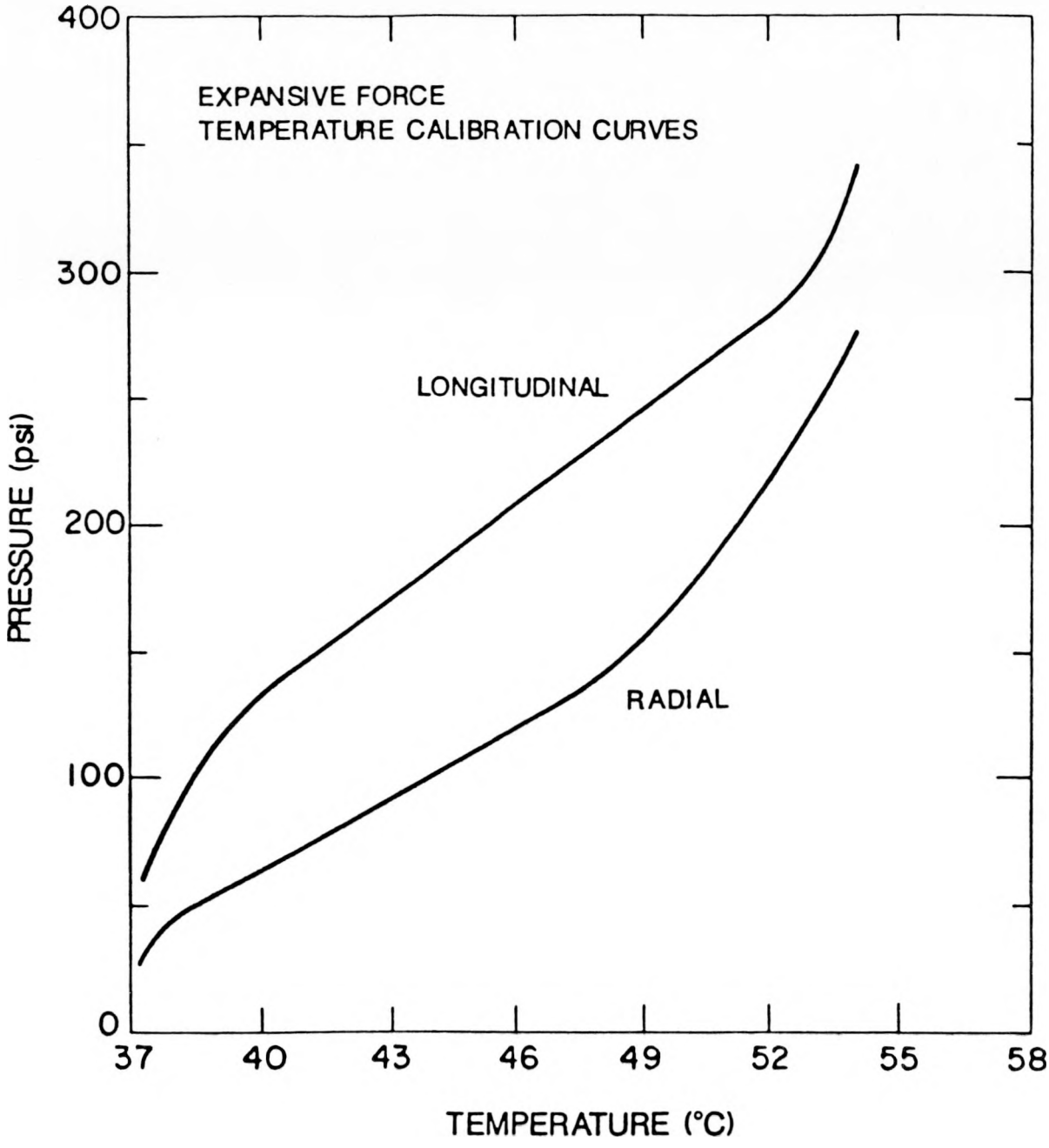

Figure B-7. Calibration Curves for Temperature Variation in Expansion Measurements

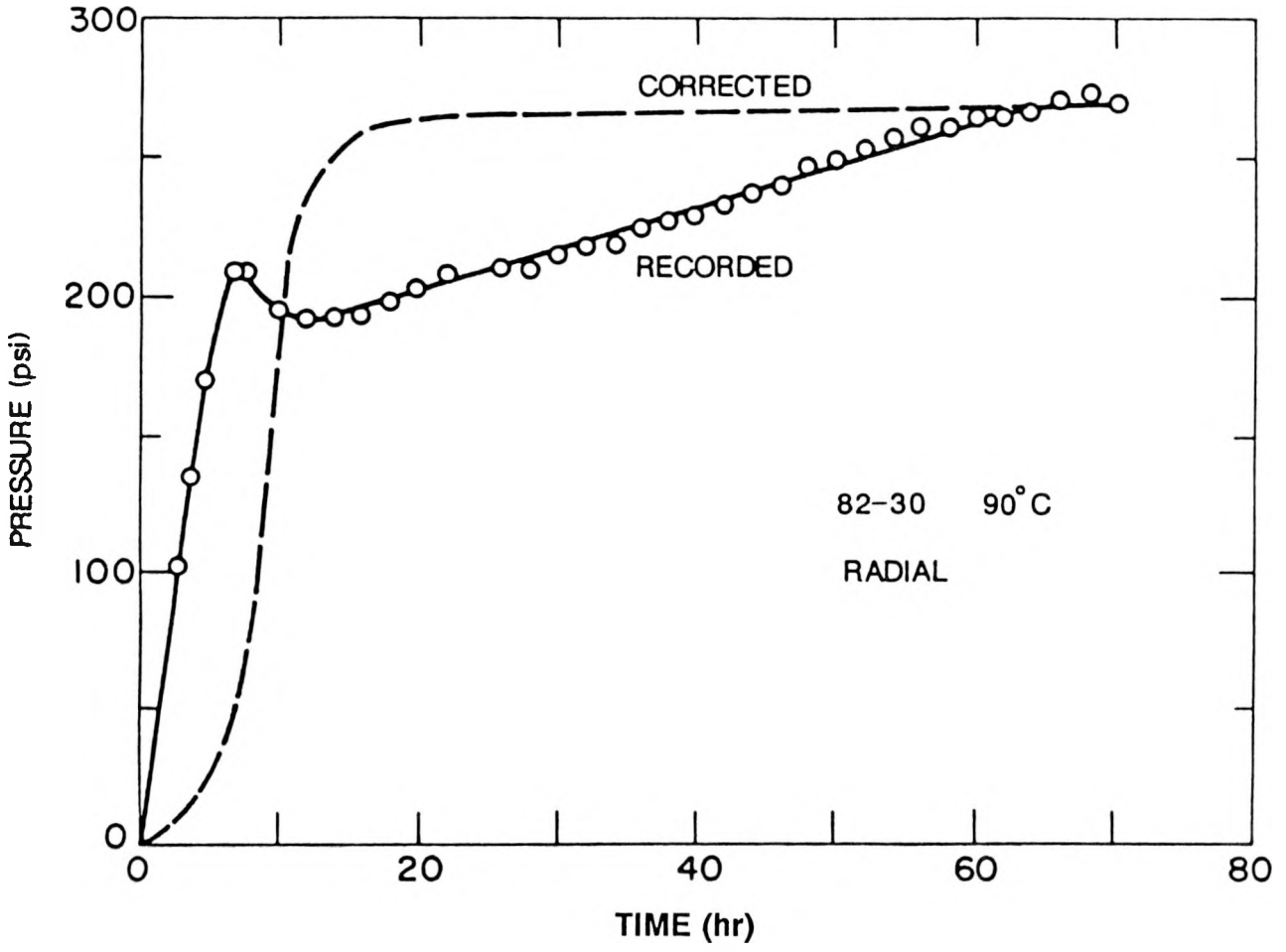

Figure B-8. Radial Expansion Curve as Recorded Compared to Corrected Curve for 90°C

B-3. BOND STRENGTH

Tuff samples were core drilled and then sawed into 2.54-cm-diameter and 2.54-m-long cylinders. One end of the tuff cylinder was abraded using air pressure of 0.55-0.69 MPa and standard alumina grit (Size 36) at about 15 cm from the surface for one minute. Each surface was then cleaned with a jet of air.

These abraded samples are placed in cylindrical brass molds that were 2.54 cm in diameter and 5.08 cm long. The surface of the tuff is wetted with a single drop of tap water before it came into contact with the cement formulation. The cement formulations, mixed according to ASTM (C 305), are poured over the tuff samples and tamped with a 3-mm-diameter rod to remove entrapped air. The molds are then covered with a flat plate and immersed in tuff ground water (E-25) and cured at appropriate temperatures for the required periods of time. In some cases the surface of the tuff interface was coated with either the Ludox sol or latex before the cement formulation was poured. A typical cement/tuff sample is shown in Figure B-9.

To set up the sample for the tensile test, the cement/tuff sample is first gripped by the upper collet assembly (Figures B-10 and B-11). The upper collet assembly is attached to a U-joint with a pin, which in turn was attached to the load cell (Figures B-12 and B-13). The chart recorder pen is then zeroed and balanced, after which a standard weight is hung from the upper collet assembly for calibration. The lower part of the sample is moved into the lower collet and gripped by tightening the screw cap (Figure B-11). In the final form, the cement paste is gripped by one assembly and the tuff by the other, about 5 mm from the interface (Figure B-12).

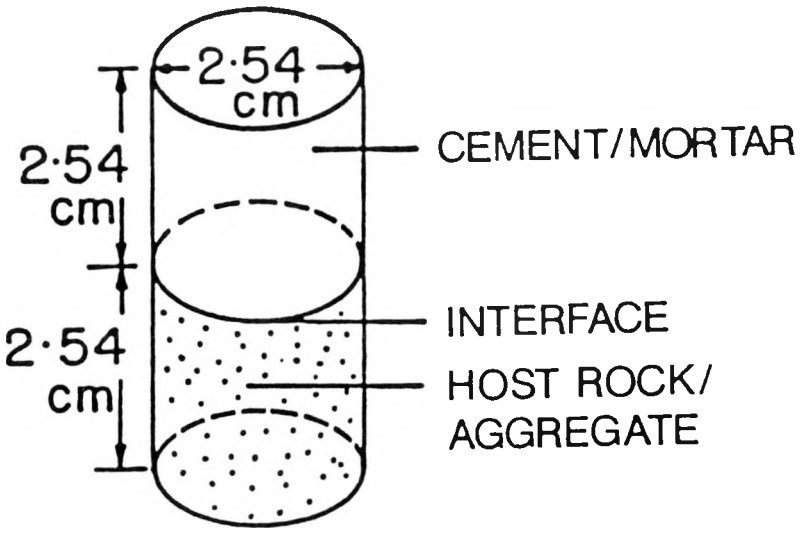

Figure B-9. A Typical Cement/Tuff Sample for the Bond Strength Experiment

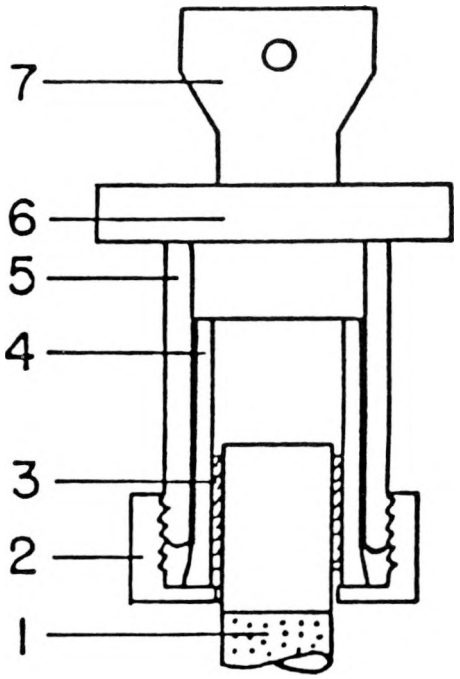

1 = sample
2 = screw cap
3 = rubber sleeve
4 = collet
5 = housing
6 = backing plate
7 = adapter

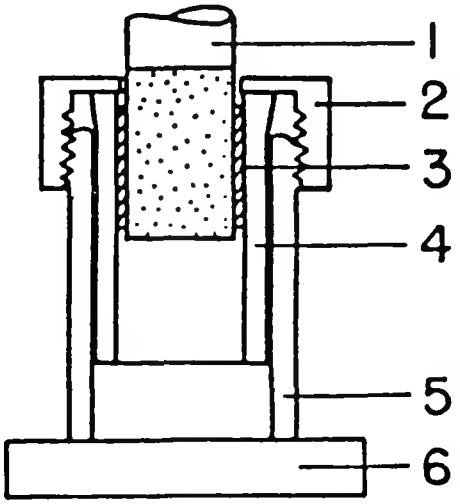

Figure B-10. Upper Collet Assembly

Figure B-11. Lower Collet Assembly

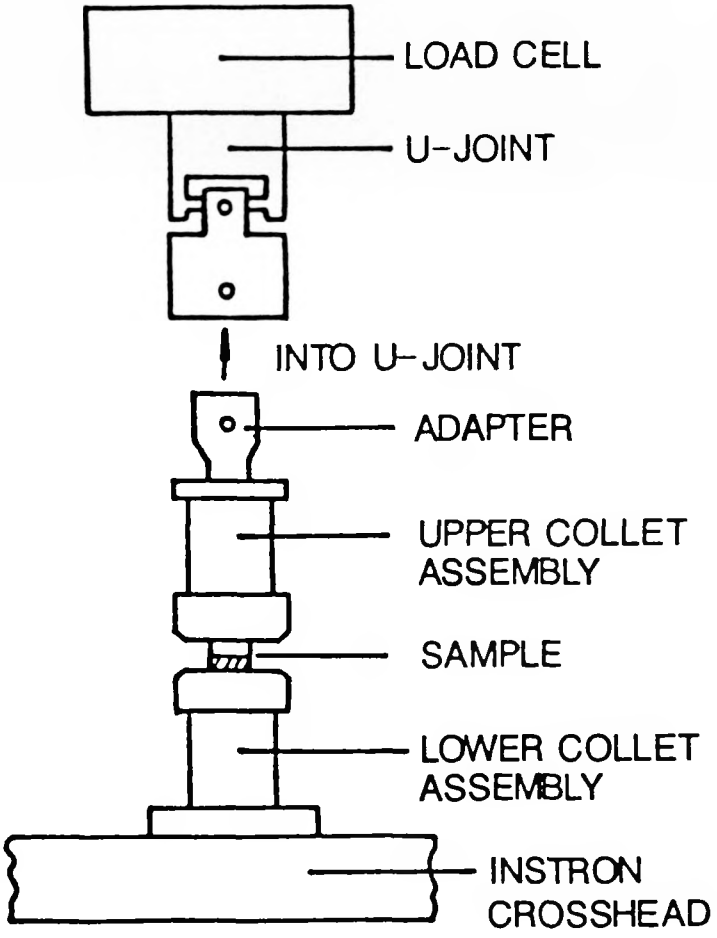

Figure B-12. Sample Setup for the Instron Showing the Position of the Upper and Lower Collet Assemblies

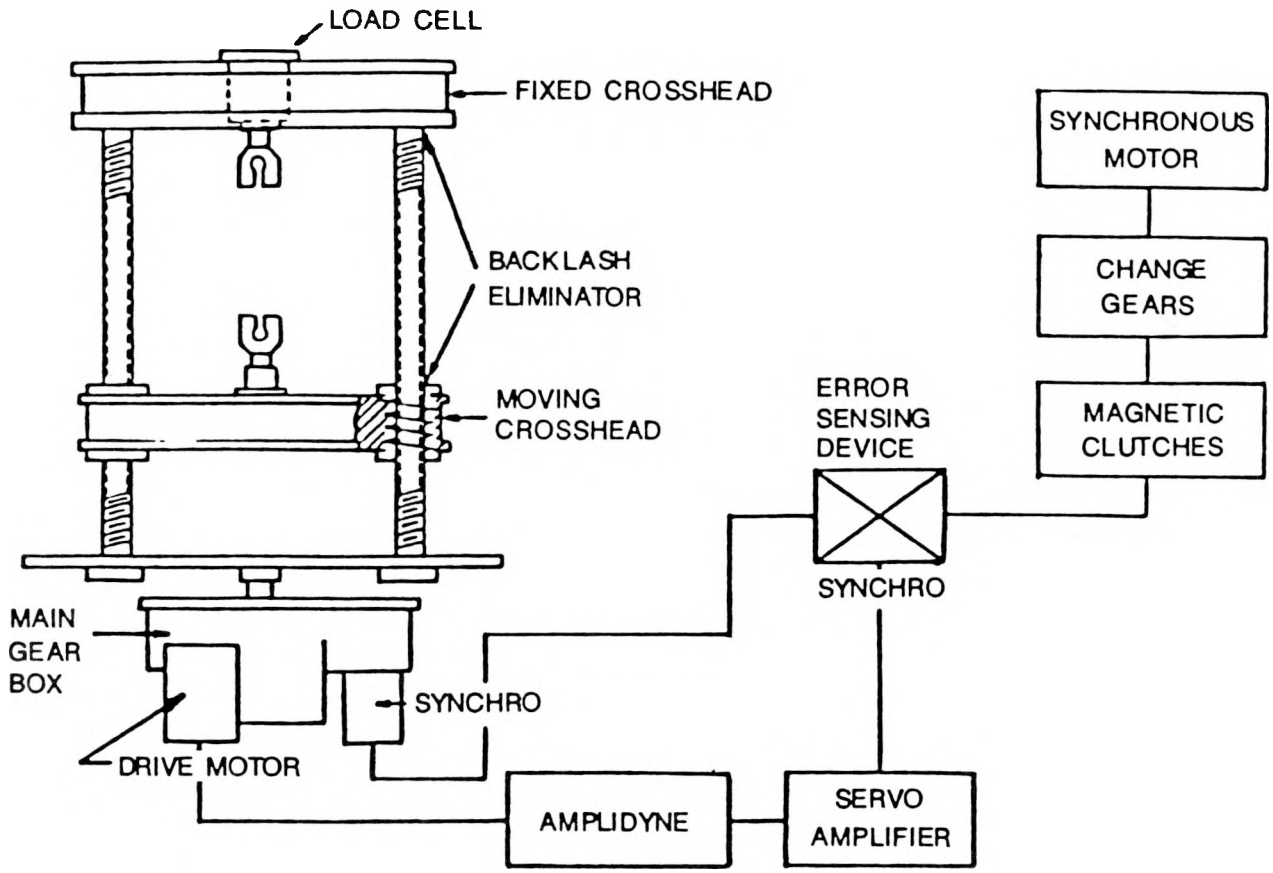

Figure B-13. Schematic Representation of the Instron Testing Machine

B-4. LIQUID PERMEABILITY

The liquid permeability apparatus consists of a sample cell, where the sample is subjected to the lateral (confining) pressure as shown in Figure B-14. The confining pressure is used to ensure that no liquid permeated along the outer cylindrical surface of the sample. The confining pressure cell is connected to a nitrogen gas cylinder and the gas pressure was set at 2 MPa. Deionized water is forced through the sample using a chromatographic pump which maintained a pressure of 1.45 MPa. The lower end of the sample is connected to a tube, from which permeating water could be collected in a reservoir resting on a sensitive linear variable differential transducer (LVDT). The LVDT is connected to a chart recorder, which recorded flow in grams of water as a function of time.

Cylindrical samples of tuff, 2.54 cm in diameter and 5.08 cm long, are sawed into hemicylinders using water as the coolant. These hemicylinders are then cleaned by washing in deionized water. The sawed surfaces are abraded in exactly the same manner as the samples for the bond strength experiment. These abraded samples are put into brass molds and cement formulations poured along the side. A typical sample configuration is shown in Figure B-15. The cement/tuff cylinders are slipped into rubber sleeves before placing them in the permeability cell. The LVDT/chart recorder is calibrated using standard weights of 25 and 100 g with scale on the chart recorder corresponding to 100 g. The samples are first confined by the nitrogen gas pressure for a few minutes, before the driving water pressure is applied. The samples are tested for 72 hr. Knowing the pressure and volume flow of water, liquid permeability is calculated (Wakeley and Roy, 1982).

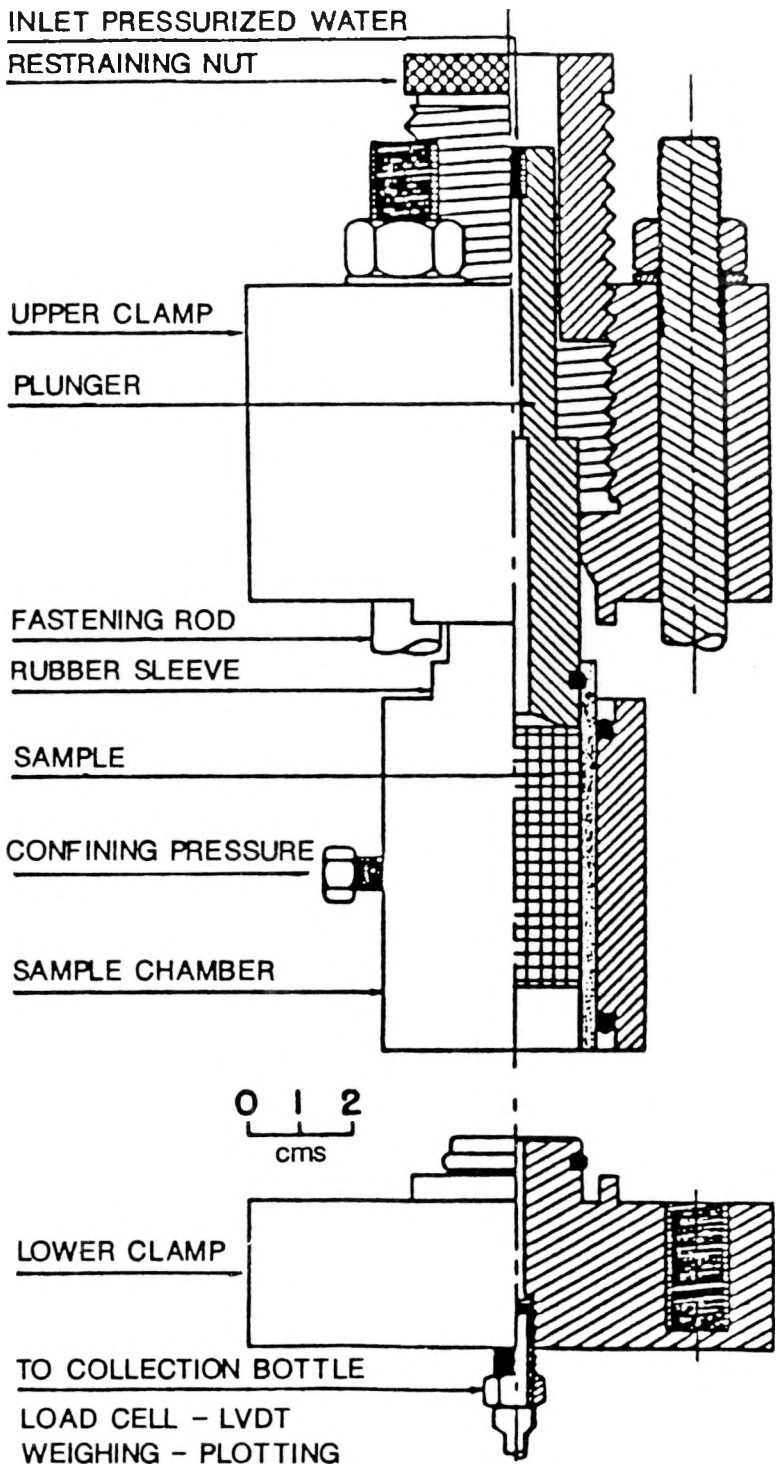

Figure B-14. Sectional View of the Liquid Permeability Apparatus

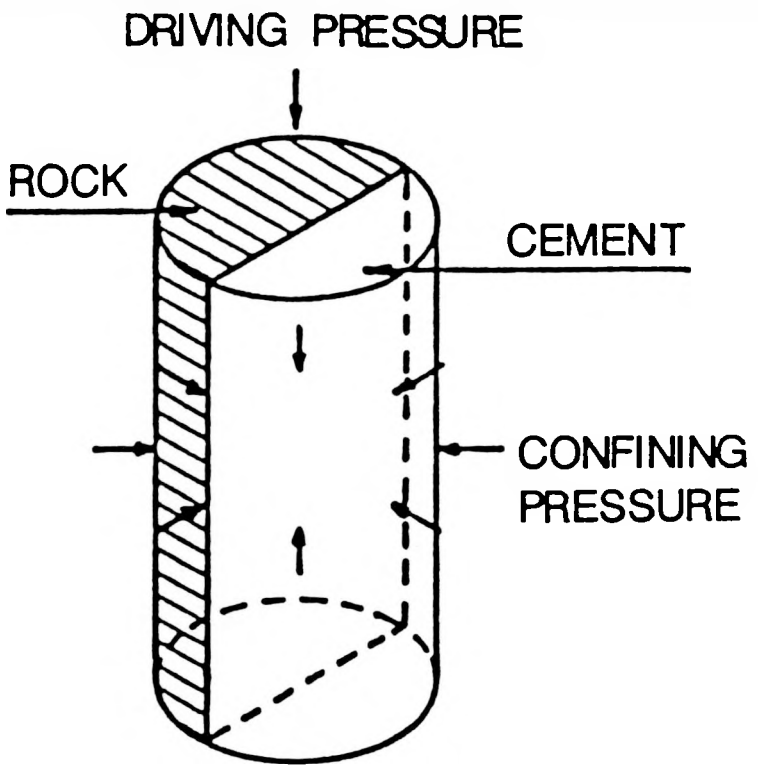

Figure B-15. Typical Cement/Tuff Samples for the Interface Permeability Studies

B-5. REFERENCES

Wakeley, L. D., and D. M. Roy, 1982, "A Method for Testing the Permeability Between Grout and Rock," Cem. Concr. Res., Vol. 12, No. 4, pp. 533-534. (NNA.890327.0040)

APPENDIX C

COMPARISON OF DATA USED IN THIS REPORT WITH THE REFERENCE INFORMATION BASE (RIB)[a]

Parameter	Section	Report Value	RIB Value[b]
Dry Thermal Conductivity			
Nonwelded tuff	3.5	<1.45 W/mK	<1.450 W/mK for PTn[c] ≤0.543 W/mK for CHn1z and CHn2z
Welded tuff	3.5	~1.4 W/mK	1.423 W/mK for TCw and TSw1 (lithophysae poor) 1.839 W/mK for TSw2
Dry Bulk Density			
for TSw2	3.4	2.22 g/cm^3	2.219 ± 0.104 g/cm^3
for tuffaceous beds of Calico Hills		1.58 to 1.87 g/cm^3	1.577 to 1.874 g/cm^3
Mean Porosity of TSw2	3.8	0.12	0.121
Mean Porosity of PTn	3.8	0.42	0.420
Mean Porosity of CHn1z	3.8	0.36	d

a. Version 4 of "The Yucca Mountain Project Reference Information Base."
b. Report values were selected during the development of the RIB. Differences in values selected in this report from values in the RIB are therefore attributable to incorporation of new laboratory and other data into the latest version of the RIB.
c. Estimate rock mass thermal conductivities given here.
d. Porosity varies with spatial location. The results are as follows:
   • UE-25a#1, USW G-4: 0.324 ± 0.037 (38) and
   • USW G-1: 0.356 ± 0.020 (6).
   Numbers in parentheses represent the number of samples measured.

APPENDIX D

DATA RECOMMENDED FOR INCLUSION IN THE SITE AND ENGINEERING PROPERTIES DATA BASE (SEPDB) AND INFORMATION PROPOSED FOR INCLUSION IN THE REFERENCE INFORMATION BASE (RIB)

No data are recommended for inclusion in the SEPDB and RIB. Data contained in this report may be reevaluated at a future time for inclusion into the SEPDB.